Journal of Affective Disorders 389 (2025) 119708

Contents lists available at ScienceDirect

Journal of Affective Disorders

journal homepage: www.elsevier.com/locate/jad

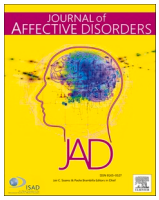

Research paper

Covarying gray and white matter networks characterize schizophrenia and bipolar disorders on a continuum: A data fusion machine learning approach and a brain network analysis

Alessandro Grecucci [a,b,*], Alessandro Scarano [a], Francesco Bruno [c], Gerardo Salvato [d], Xiaoping Yi [e,f,g,**], Massimo Stella [a]

[a] Department of Psychology and Cognitive Science, University of Trento, Italy
[b] Center for Medical Sciences, University of Trento, Italy
[c] Universitas Mercatorum, Roma, Italy
[d] Università di Pavia, Pavia, Italy
[e] Department of Radiology, Chongqing University Three Gorges Hospital, Chongqing University, Chongqing 410008, PR China
[f] Clinical Research Center (CRC), Medical Pathology Center (MPC), Cancer Early Detection and Treatment Center (CEDTC) and Translational Medicine Research Center (TMRC), Chongqing University Three Gorges Hospital, Chongqing University, Chongqing 404000, PR China
[g] School of Medicine, Chongqing University, Chongqing 400030, PR China

ARTICLE INFO

Keywords:
Schizophrenia
Bipolar disorder
Independent vector analysis
Continuum hypothesis
Data fusion
Networks

ABSTRACT

Schizophrenia (SZ) and Bipolar disorder (BD) share genetic and cerebral abnormalities, supporting an expanded continuum hypothesis. In this paper, we aim to better characterize differences and commonalities of gray and white matter features between SZ and BD to clarify how they align or diverge on this continuum. We transposed independent vector analysis (tIVA), a data fusion technique, to the gray and white matter images of 128 individuals diagnosed with SZ, 128 with BD and 127 healthy controls (CTRL), matched for gender, age and IQ. Of the 18 tIVA networks detected, three differed between SZ and BD (tIV9,14,15), primarily involving frontotemporal regions. These same networks plus two more (tIV3,4), differed between SZ and CTRL indicating a larger compromission, whereas only one network (tIV9) differed between BD and controls. Overall, SZ displayed the more pronounced GM-WM abnormalities in both extent and severity with BD lying in an intermediate position. Of note, one network differed among all three groups (SZ, BD, and CTRL). Random forest classification confirmed these results by indicating the tIV9 as the main predictors that separate the three groups. Moreover, to appreciate eventual differences between networks across the three groups a network analyses was performed. Individuals with SZ demonstrated a significantly different clustering coefficient and density compared to CTRL. While the comparison between individuals with BD and controls did not show marked differences. This study sheds new lights on the expanded continuum hypothesis according to which individuals with schizophrenia and bipolar disorder lay on the same continuum of neurological abnormalities.

1. Introduction

Schizophrenia (SZ) and bipolar disorder (BD) have long been recognized as distinct psychiatric conditions, each characterized by specific symptomatology and clinical presentations and thus have been categorized distinctly in diagnostic manuals such as the DSM-5 and ICD-10 (DSM-5; American Psychiatric Association [APA], 2013, ICD-10; World Health Organization [WHO], 1993). SZ is defined by its hallmark features of psychosis, including hallucinations, delusions, and disorganized thinking, while BD is characterized by episodes of mood disturbance, alternating between mania and depression (APA, 2013). BD and SZ, while distinct in their symptomatology, share several clinical features that can sometimes blur diagnostic boundaries and complicate accurate diagnosis (Moller, 2003; Sorella et al., 2019). These

* Correspondence to: A. Grecucci, Department of Psychology and Cognitive Science, University of Trento, Italy.
** Correspondence to: X. Yi, Department of Radiology, Chongqing University Three Gorges Hospital, Chongqing University, Chongqing 410008, PR China.
E-mail addresses: alessandro.grecucci@unitn.it (A. Grecucci), alessandro.scarano-1@unitn.it (A. Scarano), francesco.bruno@unicz.it (F. Bruno), gerardo.salvato@unipv.it (G. Salvato), yixiaoping@csu.edu.cn (X. Yi), massimo.stella-1@unitn.it (M. Stella).

https://doi.org/10.1016/j.jad.2025.119708
Received 27 March 2025; Received in revised form 3 June 2025; Accepted 14 June 2025
Available online 21 June 2025
0165-0327/© 2025 The Authors. Published by Elsevier B.V. This is an open access article under the CC BY license (http://creativecommons.org/licenses/by/4.0/).

overlapping features include mood disturbances, cognitive dysfunctions, and psychotic symptoms, which can lead to diagnostic challenges and the potential for misdiagnosis (Miller et al., 2014; Tandon et al., 2013; Grecucci et al., 2023). Whereas mood disturbances are a hallmark feature of BD, individuals with SZ may also experience mood instability (Sorella et al., 2019). Affective lability, irritability, and dysphoria can occur in SZ (Sorella et al., 2019), particularly during acute exacerbations or in the presence of comorbid mood disorders. At the same manner, psychotic symptoms such as hallucinations and delusions, typically more prominent and persistent in SZ, can also occur during manic or depressive episodes in BD (APA, 2013; CIT). Disorganized thinking and speech patterns are common in both disorders. Individuals may exhibit tangential or illogical speech, derailment (sudden shifts in topic), or thought blocking (sudden interruption of thought process) (Barch & Ceaser, 2012). Both schizophrenia and bipolar disorder are associated with cognitive impairment, although the specific cognitive deficits may vary (Barch & Ceaser, 2012). Executive function deficits, attentional difficulties, and memory impairments can occur in both disorders and contribute to functional impairment (Grecucci et al., 2023). Both schizophrenia and bipolar disorder can lead to impaired social functioning. Individuals may experience difficulties in maintaining relationships, holding employment, and engaging in daily activities (Grecucci et al., 2023). Social withdrawal, isolation, and interpersonal conflicts may occur in both disorders (Grecucci et al., 2023). Individuals with either disorder may use substances as a means of self-medication to alleviate distressing symptoms or to cope with social isolation and stigma (Khantzian, 1997; Regier et al., 1990). Literature suggested that there are also some *common neurobiological features* observed in both disorders. SZ and BD share a range of neurobiological features, suggesting a significant overlap between these conditions. Common elements include disruptions in dopamine and glutamate systems, neurodevelopmental abnormalities, and inflammatory processes, all of which contribute to the symptomatology observed in both disorders (Craddock and Owen, 2010; Moghaddam and Javitt, 2012; Goldsmith et al., 2016). Genetic studies have further revealed shared risk factors, indicating that these disorders may arise from similar underlying biological mechanisms (Sullivan et al., 2012; Sorella et al., 2019; Grecucci et al., 2023).

From an affective point of view, multiple commonalities are also present. Deficits in emotion regulation and emotional instability linked to fronto-limbic alterations are well-established in BD, as highlighted in the review by Townsend and Altshuler (2012). In contrast, SCZ patients exhibit impairments across various emotional domains, including experiencing, perceiving, recognizing, and expressing emotions (see reviews by Aleman and Kahn, 2005; Kohler and Martin, 2006; Trémeau, 2006). Additionally, they display abnormalities in emotional memory, particularly intrusive and negative memories (Herbener, 2008), which can shape the content and interpretation of hallucinations (Laloyaux et al., 2019; Waters et al., 2012). This has been recently confirmed by a large metanalysis of fMRI studies on emotional perception comparing SCZ with BD (Grecucci et al., 2023). This study revealed shared functional abnormalities in the thalamus, parahippocampal regions, and basal ganglia, indicating that these patients exhibit disruptions in a neural circuit involved in the intensified processing of negative emotional stimuli (Grecucci et al., 2023).

These findings have led to the hypothesis of a continuum between SZ and BD, suggesting common genetic vulnerabilities that lead to shared psychotic symptoms, while other genetic and environmental factors contribute to the disorders' differentiation (Expanded continuum hypothesis, Sorella et al., 2019). This hypothesis suggests that both disorders share a continuum of psychotic symptoms, including hallucinations and delusions, albeit with differing clinical presentations and severities (Sorella et al., 2019). For instance, while SZ is characterized by persistent and prominent psychotic symptoms, BD may exhibit these symptoms primarily during manic or depressive episodes (APA, 2013). Neuroimaging studies support this continuum hypothesis by showing overlapping abnormalities in brain structure and function. Neuroimaging studies using Voxel-based Morphometry (VBM) have found significant gray matter overlaps in SZ and BD patients, particularly in the prefrontal, subcortical, temporal, and parieto-occipital areas, compared to healthy controls. However, direct comparisons indicate more pronounced impairments in SZ, particularly in the frontal gyri, temporal gyri, and insula (Maggioni et al., 2017; Nenadic et al., 2015; Rimol et al., 2012; Molina et al., 2011; Bowie et al., 2020; McLaughlin et al., 2017; Bora and Pantelis, 2015; Bortolato et al., 2015; Lewandowski et al., 2011; Bowie et al., 2020). However, these studies are limited as they typically compare SZ and BD indirectly against healthy controls using univariate methods like VBM, which do not fully capture the relationships between different brain voxels (Mcintosh et al., 2004; Arnone et al., 2009; Yu et al., 2010; Ellison-Wright & Bullmore, 2010). To overcome these limitations, Source-based Morphometry (SBM) was proposed as a more comprehensive method for studying psychiatric disorders from a whole-brain and network perspective (Grecucci et al., 2016, 2017; Pappaianni et al., 2018). In particular, Sorella et al. (2019) presented a detailed exploration of the similarities and differences between SZ and BD, introducing SBM as a method to investigate these disorders comprehensively, aiming to expand the understanding of the continuum hypothesis by examining shared and distinct neural and psychological mechanisms in SZ and BD. SBM is part of machine learning techniques that have become increasingly prominent in neuroscience due to their ability to explore complex relationships among brain variables, such as individual voxels. Unlike traditional univariate analyses, which examine each voxel in isolation, these multivariate approaches enable the simultaneous analysis of multiple voxels, revealing subtle and distributed changes in brain structure and function (Grecucci et al., 2022; Hebart & Baker, 2018; Vieira, Pinaya, & Mechelli, 2020).

Considering these premises and the expanded continuum hypothesis, this study aims to further investigate the differences and commonalities of gray and white matter features between SZ and BD by employing machine learning methods. We hypothesize that SZ and BD will share common gray matter (GM) and white matter (WM) networks that are significantly different from healthy controls, supporting the existence of a shared psychotic core as suggested by the continuum theory. Specifically, we anticipate identifying at least one network that distinguishes both SZ and BD from controls. Furthermore, we propose that SZ patients will exhibit greater abnormalities in networks associated with cognitive functions, such as fronto-parietal circuits, compared to BD patients and healthy controls. This would reflect the more severe cognitive impairment often observed in SZ. Conversely, we predict that BD patients will show specific alterations in networks related to affective processing and mood regulation, distinguishing them from SZ patients and controls. These alterations may be evident in limbic and prefrontal regions involved in emotional regulation, such as the amygdala, hippocampus, and ventromedial prefrontal cortex. This would suggest a distinct affective core in BD, characterized by disruptions in emotional processing circuits. Consistent with the continuum hypothesis, we also expect that the SZ group will display the most pronounced GM-WM abnormalities, both in terms of the number of affected networks and reduced matter concentration. BD patients are anticipated to show intermediate levels of impairment, standing between SZ patients and healthy controls. This gradient of abnormalities aligns with the notion of a spectrum of severity across these disorders, where BD occupies a middle position along the continuum from healthy controls to SZ.

To test these hypotheses, in the present study, unsupervised machine learning techniques, specifically Transposed Independent Vector Analysis (tIVA), were employed to identify independent neural circuits (Adali et al., 2015; Lee et al., 2008). Transposed Independent Vector Analysis (tIVA) was selected because it combines the strengths of independent component analysis and canonical correlation analysis among current data-driven fusion families while avoiding their core limitations. In contrast to joint-ICA, which forces all modalities to share a single

mixing matrix and therefore presumes equal contributions from each signal (Calhoun et al., 2006), tIVA keeps a separate mixing matrix per modality yet couples the source vectors statistically, permitting shared variance to emerge without imposing identical spatial distributions. Relative to multiset-CCA or mCCA + jICA (Sui et al., 2013), the tIVA likelihood incorporates higher-order (non-Gaussian) statistics, giving higher sensitivity to subtle, non-linear cross-modal relationships that are characteristic of psychosis-related brain alterations. Benchmark studies in multimodal schizophrenia samples have shown that tIVA yields more stable components and higher diagnostic-classification accuracy than linked-ICA or joint-ICA while scaling linearly in computation as additional modalities are added (Adali et al., 2015). Finally, because tIVA models independence within each modality but explicit dependence across modalities, it preserves modality-specific information (e.g., gray vs. white-matter concentration) that might otherwise be lost in approaches that concatenate or down-sample the data (Groves et al., 2011). For the present question, isolating covarying GM–WM networks that discriminate schizophrenia, bipolar disorder, and controls, this ability to separate, yet link, sources made tIVA uniquely well-suited.

tIVA reduces the complexity of brain data, which typically includes around 100,000 voxels, by organizing it into a smaller number of biologically meaningful networks (Baggio et al., 2023; Grecucci et al., 2022). These networks are considered more biologically relevant than traditional atlas-based brain maps, which are based on anatomical or histological features rather than functional or temporal interactions between regions (Biswal et al., 2010; Fox et al., 2005). This method aligns with the understanding that personality traits are associated with multiple brain networks rather than a single specific area. Furthermore, the analysis included both gray and white matter features in a data fusion approach because both can provide valuable insights and may be influenced by similar genetic factors (Spalletta et al., 2018; Baggio et al., 2023). White matter, which is often studied using diffusion tensor imaging (DTI), is critical because pathological processes affect it as well as gray matter (Assaf & Pasternak, 2008; Alba-Ferrara & de Erausquin, 2013). DTI measures the movement of water molecules to assess white matter integrity but is highly sensitive to noise, which can affect the reliability of results (Radwan et al., 2022). A combined approach that considers both gray and white matter allows for a more comprehensive evaluation of brain alterations without the limitations associated with focusing solely on specific white matter tracts (Baggio et al., 2023).

Additionally, a supervised machine learning technique was applied, specifically Random Forest classification, to build a predictive model capable of classifying individuals into their respective groups based on the identified networks. This approach not only contributes to our understanding of the underlying brain abnormalities but also offers a predictive framework for potential clinical applications. Moreover, to examine the differences in brain connectivity between the groups more thoroughly, we conducted a comprehensive brain network analysis, inspired by (Sporns, 2016), on the loading coefficients derived from the tIVA. By constructing individual brain networks based on the relationships between the independent components (tIVs) for each participant, we examined how these networks are organized and connected in SZ, BD, and control participants. This analysis involved assessing network metrics such as clustering coefficients and network density, which provide insights into the efficiency and integration of neural networks. By comparing these metrics across groups, we aimed to identify specific alterations in brain network architecture that distinguish SZ and BD, potentially revealing unique connectivity patterns associated with each disorder within the continuum framework.

By integrating these advanced analytical approaches, our study aims to provide a deeper understanding of the neural underpinnings of SZ and BD within the expanded continuum hypothesis. Identifying both shared and distinct neural circuits may help clarify the boundaries and overlaps between these disorders, with important implications for diagnosis and the development of targeted interventions based on specific neural alterations. Ultimately, we hope to contribute to a more integrated understanding of these complex psychiatric conditions, enhancing diagnostic accuracy and informing personalized treatment strategies.

2. Methods

2.1. Participants

This study capitalizes on the brain scans of 383 participants selected collected by Salvador et al. (2017). The participants were divided into three different groups. The first group consisted of 128 individuals diagnosed with schizophrenia based on DSM-IV criteria, selected from two hospitals in Spain: Benito Menni CASM and Mare de Déu de la Mercè. The second group included 128 patients with type I bipolar disorder from Benito Menni CASM and Hospital Clínic de Barcelona, matched with the first group for age, gender, and premorbid IQ. Premorbid IQ was estimated using the Word Accentuation Test (proper citation needed here). At the time of scanning, among the bipolar disorder patients, 77 were in a state of euthymia (a clinically stable condition, neither manic nor depressed), 28 were in a manic phase, and 23 were in a state of depression (see Salvador et al., 2017 for a complete report). The third group comprised 127 healthy control individuals, drawn from non-medical hospital staff and the general community, who were matched using the same criteria and had no reported history of mental illness or treatment with psychotropic drugs. All patients were further assessed using the PANSS (SZ mean = 72.6; BD mean = 46), while bipolar patients were additionally evaluated with the YMRS (mean = 5.95) and the HDRS (mean = 7.43). See Salvador et al. (2017) for a complete report. All participants were right-handed, aged between 18 and 65 years, and shared the same exclusion criteria: no history of brain trauma or neurological disease and no alcohol or substance abuse in the last 12 months prior to their brain scan.

Further demographic and clinical details of the three samples are presented in Table 1. The study received ethical approval from the

Table 1
Modified from Salvador et al. (2017). Demographic and Clinical Characteristics of Study Participants.

	Schizophrenia	Bipolar disorder	Controls	*p*-values
Participants	128	128	127	
Age	41.5 (10.3) Range: 18–65	41.4 (10.4) Range: 20–64	39.8 (10.3) Range: 20–64	p(sz, bd) = 0.94 p (sz, ctrl) = 0.18 p (bd, ctrl) = 0.21
Gender	F = 54, M = 74	F = 54, M = 74	F = 54, M = 73	p(sz, bd = 1.0 p (sz, ctrl) = 0.96 p (bd, crl) = 0.96
WAIS-III	91.9 (17.6)	93.4 (15.6)	107.2 (15.5)	p(sz, bd) = 0.51 p (sz, ctrl) < 0.0001 p(bd, ctrl) < 0.0001
Exclusion criteria	Brain trauma, Neurological disease, Alcohol/ substance abuse in the last year	Brain trauma, Neurological disease, Alcohol/ substance abuse in the last year	Brain trauma, Neurological disease, Alcohol/ substance abuse in the last year, History of mental illness, Treatment with psychotropic medication	

Comité de Ética de Investigación Clínica de las Hermanas Hospitalarias. Informed written consent was obtained from all participants, which detailed the study's procedures and the intended use of the data.

2.2. Image acquisition

For this study, structural brain images were acquired using a 1.5-T GE Signa scanner (General Electric Medical Systems, Milwaukee, WI, USA). The specific parameters chosen for the T1-weighted sequence were as follows: 180 axial slices with a 1 mm slice thickness and no gap, a 512 × 512 matrix size, and a 0.5 × 0.5 × 1 mm^3 voxel resolution. The sequence also had an echo time (TE) of 4 ms, a repetition time (TR) of 2000 ms, and a 15° flip angle.

2.3. Pre-processing

SPM12's unified segmentation algorithm (Ashburner, 2009), was used to segment the images into gray and white matter partial volume images. The brain-extraction process, as described by Smith (2002), was followed by alignment to the MNI152 standard template at 2 mm resolution using FSL registration tools (Jenkinson et al., 2012). The DARTEL deformation fields obtained from this alignment were applied to the segmented images to generate normalized gray and white matter images, which were then subsampled to a 4 × 4 × 4 mm^3 resolution to reduce computational cost.

2.4. Unsupervised machine learning to decompose the covarying GM-WM networks

In this study, we employed a novel unsupervised machine learning technique known as Transposed Independent Vector Analysis (tIVA) (Adali et al., 2015; Lee et al., 2008) to decompose the brain into independent neural circuits from the structural magnetic resonance imaging (sMRI). Fusion ICA Toolbox (FIT, http://mialab.mrn.org/software/fit) (Calhoun et al., 2006) within MATLAB 2018a (https://it.mathworks.com/products/matlab.html) (MATLAB (R2018a)), was used to perform tIVA on the preprocessed GM and WM images. To determine the optimal number of independent vectors, the MNL algoritm was used. We further assessed the reliability of each modality by employing the ICASSO GIFT toolbox (Himberg et al., 2004), iterating the Infomax algorithm 100 times. The output was organized into a matrix with subjects as rows and components as columns, where the loading coefficients represented the extent of each subject's gray and white matter concentration within the individual components. These independent vectors were then translated into Talairach coordinates to facilitate the identification of the associated brain regions. Positive and negative brain region values were included as necessary. We visualized the networks using Surf Ice (https://www.nitrc.org/projects/surfice/) (Rorden), which provided us with a spatial representation of the components. For statistical analysis, independent sample *t*-tests in Jasp version 0.16.3 (Jasp Team (Version 0.16.2) (2023)) to the loading coefficients was used to discern any significant differences across groups. This approach helped us to understand the specific contributions of each network component to the conditions under study.

2.5. Supervised machine learning to build a predictive model

In order to derive a predictive model to classify the three groups, we performed a Random Forest classification on the loading coefficients of the tIVs. This may be informative of the fact that at least some brain networks are able to separate the three groups. Random forest is an ensemble learning method for classification that operates by constructing a multitude of decision trees and averaging their performance using the bagging method (Ho, 1998; Breiman, 2001). This machine learning method was selected due to its robust performance in classification tasks and its inherent capacity to minimize overfitting (outperforming decision trees and other SML algorithms)—a common challenge in machine learning (Hastie et al., 2001). To implement the Random Forest, we configured an ensemble of trees and employed cross-validation to fine-tune the hyperparameters, ensuring the model's generalizability. Each tree in the forest received the GM network coefficients as input and contributed a vote towards the classification of a subject (e.g., BPD patient, SZ patient, or healthy control). The final classification is determined by a majority vote, with trees weighted according to their predictive accuracy. 5000 permutations were used to assess the reliability of the model. Of note, the random forest method is able to determine the importance of each feature (neural networks defined by the tIVs).

2.6. Network analysis

We used brain network science to investigate the data from another perspective. Brain network science is a field rapidly growing at the intersection of network science and neuroscience (Sporns, 2016). Inspired by past approaches in the field (Zalesky et al., 2012), we built complex networks out of differences in expression levels across all pairs of tIVs. In other words, a comprehensive network analysis was conducted on the loading coefficients data from the 3 groups of patients. For each subject, the loading coefficients of the 18 tIVs were considered. For every patient, a subtraction matrix was then constructed, checking the absolute values of differences in expression levels between any two investigated tIVs. Every matrix had a dimension of 18 × 18, and it numerically encoded the differences in coefficients between brain regions for a given individual. We thus considered a total of 128 + 128 + 127 matrices. As suggested in (Zalesky et al., 2012), we then translated each numerical matrix into a binary adjacency matrix, checking whether the differences were below a target threshold T and connecting any two brain regions i and j whose difference in activation signals was higher than T. Through a qualitative analysis of shape, a threshold $T = 0.07$ was identified as a tipping point in the distribution of weighted differences across all individuals (cf. Supplementary Fig. 1), separating most of the lower activation differences from higher values. For every individual, every value in their related numerical matrix lower than $T = 0.07$ was set to zero, and values exceeding $T = 0.07$ were set to one.

These binary matrices served as the individual adjacency matrices for building simple graphs, i.e. unweighted, loop-less and undirected, complex networks where nodes represent brain regions, numbered from 1 to 18 for the sake of visualization, and connections indicate that any two brain regions have a difference in activation levels stronger than the selected T. We understand that this binary approach has the limitation of depending on the selection of T (Sporns, 2016). For this reason, we replicated the analyses for 3 other values of T (0.01, 0.03 and 0.1) emerging as potential tipping points. The $T = 0.1$ led to networks being disconnected >90 % of the times, indicating that this value was too restrictive and was thus discarded. In the Results we present and compare outcomes for cases $T = 0.07$, $T = 0.03$ and $T = 0.01$.

To better assess the structure of individual-level networks, two network measures of relevance in psychological networks (Castro and Stella, 2019) were calculated: the mean local clustering coefficient and network density.

We selected these two measures because they offer fundamental and complementary insights into network topology. The mean local clustering coefficient provides a measure of local network structure and the tendency of nodes to form tightly connected clusters, reflecting functional segregation. This is particularly relevant as alterations in local information processing have been implicated in both schizophrenia and bipolar disorder (e.g., how efficiently nodes within a local neighborhood communicate). Network density, in contrast, offers a global perspective on the overall connectedness of the network, indicating the extent of integration across all identified components. This allows for an assessment of widespread changes in brain connectivity. While numerous other topological measures exist, we prioritized these two as they are

well-established, provide interpretable insights into both local and global aspects of network organization (Sporns, 2016; Rubinov and Sporns, 2010), and are particularly informative for an initial characterization of differences in networks derived from structural covariance data.

Specifically, the mean local clustering coefficient measures how locally a graph contains all possible connections between nodes. More in detail, the mean clustering coefficient is the mean of the local fraction of nodes being neighbors of a given node *i* being linked with each other. The mean is computed arithmetically over all the *N* nodes in a network. This mean local clustering coefficient *C* ranges between 0 and 1 and it can be expressed mathematically as:

$$C = \sum_{i=1}^{N} \frac{c_i}{N}, c_i = \frac{2|j,k \in \partial_i, (j,k) \in E|}{|\partial_i|(|\partial_i| - 1)},$$

where c_i is the local clustering coefficient of node *i*, ∂_i is the set of all nodes linked to node *i*, *E* is the edge list containing all generic edges, e.g. (j,k), between nodes in the network. A higher mean local clustering coefficient indicates a higher chance for any two neighbors of a node to be connected with each other (Newman, 2018). In brain networks, a higher clustering can indicate the co-activation of different brain regions for a given measurement window (Sporns, 2016).

Network density evaluates the ratio between the number $|E|$ of existing connections in a network and the maximum number of possible connections, in formulas:

$$d = \frac{2|E|}{N(N-1)}.$$

We computed these structural network measures for every individual in the three considered clusters of individuals with schizophrenic disorder, bipolar disorder, and control individuals. To discover whether there were structural differences in the way tIVs coefficients differed between brain regions among the three groups we pursued additional statistical analyses. Statistical differentiation for these two measures among the groups was pursued using the Mann-Whitney *U* test, having fixed a confidence level of 0.05. This non-parametric test was chosen to compare the different ranks of network measures for the unpaired groups without having to deal with violations of the normality assumption.

3. Results

3.1. tIVA results

The Transposed Independent Vector Analysis (tIVA) estimated 18 independent covarying gray matter (IC-GM) and white matter (IC-WM) networks. See Supplementary Fig. S1 for a graphical representation of each network. The statistical significance of the identified networks was initially assessed using One-way ANOVA and then *t*-tests in JASP to compare the loading coefficients between groups. One way ANOVA returned a significant model ($F(2,380) = 14.563$, $p < 0.001$, $\eta^2 = 0.071$, SZ mean = 0.789, SD = 0.66, BD mean = 0.811, SD = 0.66, CTRL mean = 0.831, SD = 0.55*),* and the simple mean groups contrasts were significant too (SZ vs BD: t-2.866, $p_{bonferroni} = 0.013$, SZ vs CTRL: $t = -5.393$, $p_{bonferroni} < 0.001$, BD vs CTRL: $t = -2.533$, $p_{bonferroni} < 0.035$). The t-test results for each tIV are detailed below, with the most significant findings graphically represented in Figs. 1,2,3,4. For Figs. 1 to 4, the brain plots were generated using SurfICE. See also Tables 2,3,4,5,6. Individuals with SZ differ from BD for tIV14($t = -4.396$,$p = 0.0001$), tIV15($t = -3.511$,$p = 0.001$), tIV9($t = -3.260$,p = 0.001). The other tIVs did not survive Bonferroni adjusted threshold of $p < 0.002$. For what concerns the comparison between SZ and CTRL the following components differed: tIV9 ($t = -7.789$, p = 0.0001), tIV14 ($t = -5.550$, p = 0.0001), tIV15 (t = −5.550, p = 0.0001), tIV4 ($t = -4.206$, p = 0.0001), tIV3 ($t = -3.400$, p = 0.001). The other tIVs did not survive Bonferroni adjusted threshold of $p < 0.002$. Last but not least, individuals with BD differed from CTRL for tIV9 ($t = -4.411$, p = 0.0001). The others were not statistically significant, $p > 0.05$. Notably, the tIV9 network demonstrated the most significant divergence across all three comparisons, suggesting a common role for both individuals with SZ and BD. Moreover, the GM-WM concentrations followed a clear trend for which individuals with SZ display the most severe reduction compared to both BD and CTRL, with BD standing in the middle of the continuum. See Supplementary Fig. S2 for a direct comparison of the loading coefficients of each network for each group.

Tables 2,3,4,5,6. Tables detailing the brain areas, Brodmann classification, volume of matter concentration, and peak coordinates provides an anatomical context of the most important networks to our results, which are instrumental in elucidating the neural underpinnings of schizophrenia and bipolar disorder.

3.2. Random forest results

The random forest classification was applied to discern patterns among schizophrenic (SZ), bipolar (BIP), and control (CTRL) subjects. Utilizing the holdout method, models were trained on 60 % of the sample, validated on 20 %, and tested on the remaining 20 %. The model achieved an average test accuracy of 68.4 % (SZ = 75 %, BD = 68.4 %, CTRL = 61.8 %). The Receiver Operating Characteristic (ROC) curve analysis, which assesses the diagnostic ability of the classifier, indicated an Area Under Curve (AUC) scores of 0.700 for all comparisons, with 0.828 for SZ, 0.636 for BD, and 0.637 for CTRL. Results indicated that the tIV9 was a key predictor within the model, signifying its prominent role in differentiating between the clinical and control groups. This aligns with the earlier tIVA results, where the tIV9 network showed significant variation across all comparisons, underscoring its potential as a biomarker for neural differences in these conditions. See Fig. 5 for a comprehensive visual representation of the model's performance (ROC, OOB), feature importance and node purity.

3.3. Network analysis

The results of the structural analysis via individual networks (see Methods) highlighted interesting pattern differentiating groups. Having fixed a significance level of 0.05, schizophrenic patients demonstrated a different clustering coefficient (*p*-value = 0.0437) and network density (0.0016) compared to controls. A similar difference was found in terms of density between patients with bipolar disorder and controls (0.0101). No difference between the mean local clustering coefficient was found between the control and bipolar disorder groups. No significant differences were observed between individuals with schizophrenic disorder and the ones with bipolar disorder. As suggested also in Fig. 6, setting the threshold at 0.07 revealed a structure consistent across >95 % of the individuals from all three groups, where areas 6 and 9 are connected to most other nodes. For its persistence across groups and individuals, we considered this structure as a network skeleton, i.e. a network structure whose presence is common and can be overlayed with additional connections, see also (Newman, 2018). This skeleton might represent a common baseline neural architecture shared among all participants, regardless of diagnostic category. Recognizing the potential limitations of a single threshold, additional analyses were conducted using two alternative thresholds, specifically at 0.01 and 0.03. Both these thresholds resulted in networks showcasing significant differences in clustering and density values between control groups. When the threshold was set at 0.03, we retrieved the same significant differences identified in the 0.07 case for the mean local clustering, although the median values for the considered network structures flipped between the 0.07 threshold (controls' networks had a median of mean local clustering higher than the one for the schizophrenic group) and the 0.03 threshold (controls' networks had a median of mean local clustering lower than the one for the schizophrenic group). These changes indicate that the

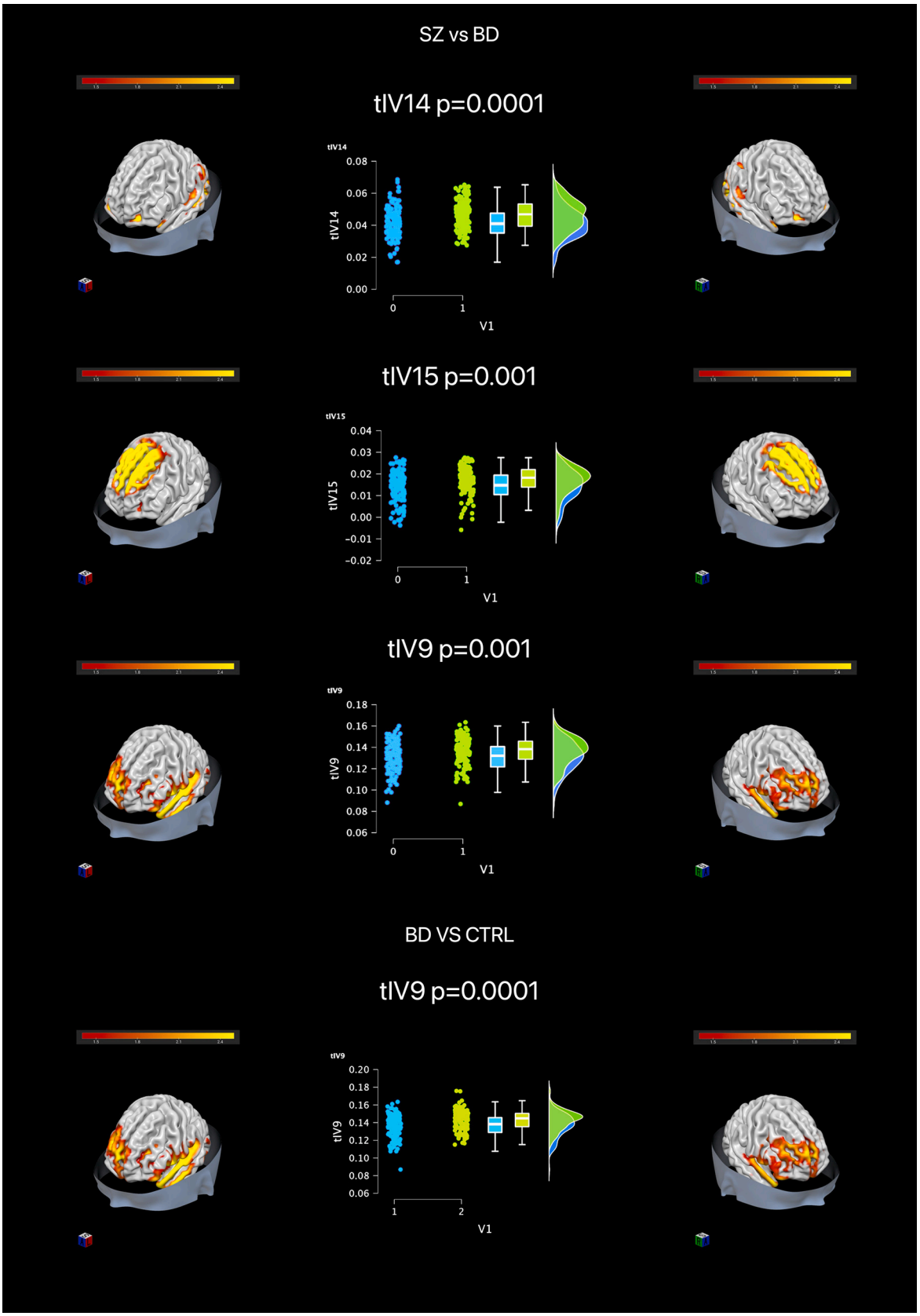

Fig. 1. Graphical representation of the gray matter areas for the most significant networks, illustrating the *t*-test results for comparisons between Schizophrenic vs. Bipolar, and between Bipolar vs. Control patients.

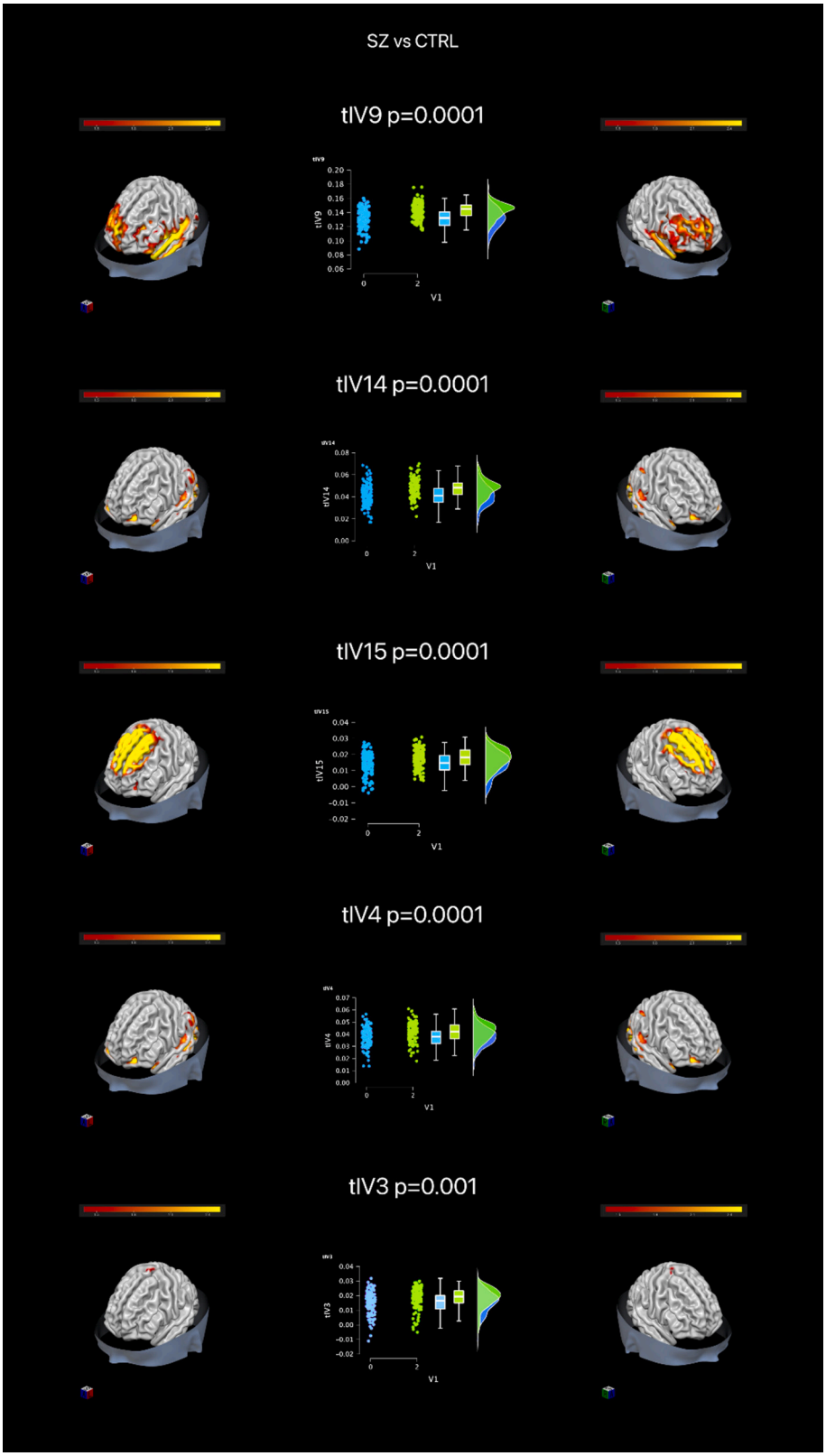

Fig. 2. Graphical representation of the gray matter areas for the most significant networks, illustrating the t-test results for comparisons between Schizophrenic and Control patients.

median values depend also on the threshold, so that the interpretation of our results should rather be relative to identifying differences from the statistical tests, as the latter limit themselves to observing differences in the mean rank of data but cannot provide insights over the medians. Always at $T = 0.03$, the networks for bipolar individuals displayed network densities compatible with healthy controls but different from patients with schizophrenic disorders (see Supplementary Table S1). Instead, individuals with schizophrenic disorders displayed networks

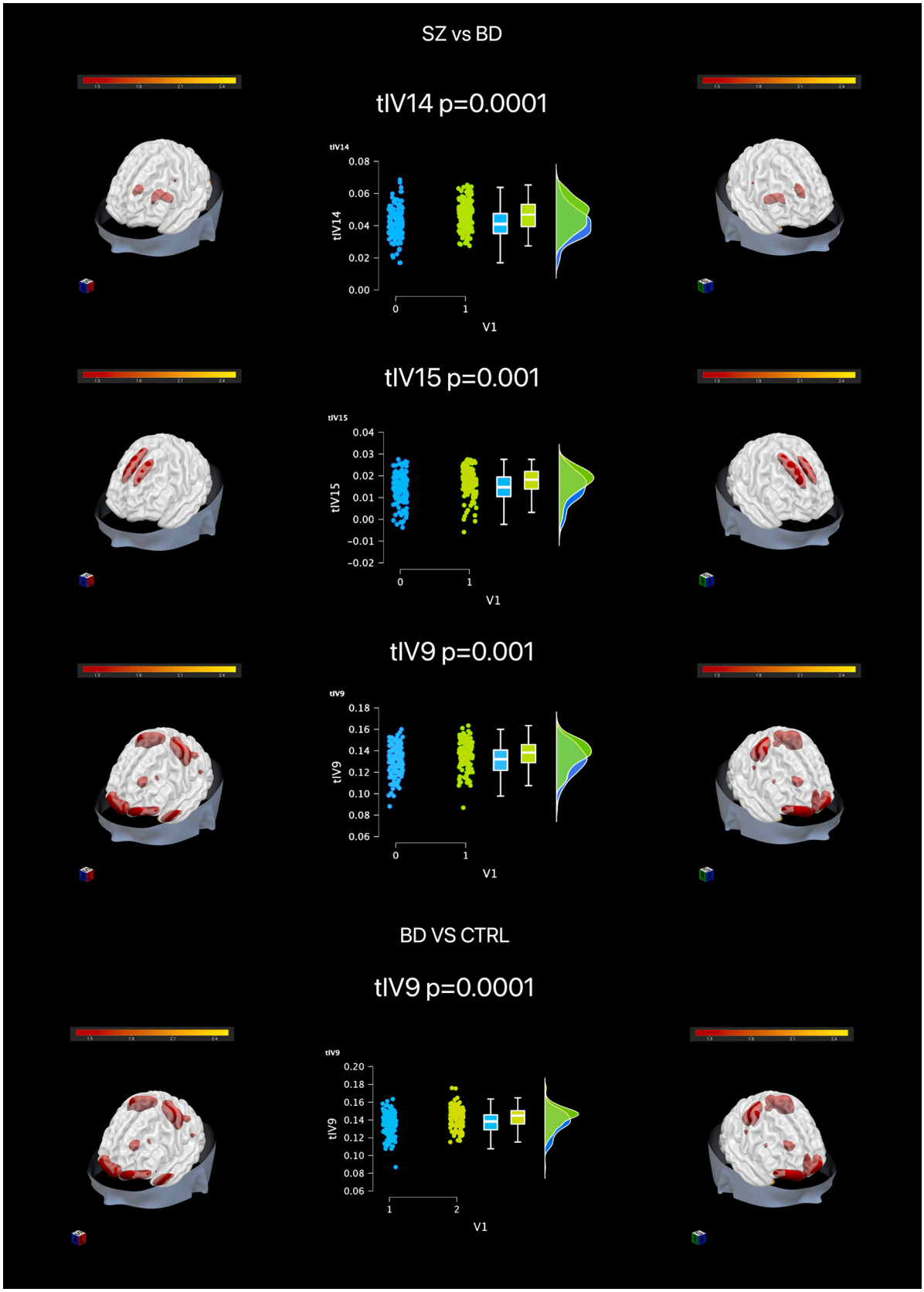

Fig. 3. Graphical representation of the white matter areas for the most significant networks, illustrating the t-test results for comparisons between Schizophrenic vs. Bipolar, and between Bipolar vs. Control patients.

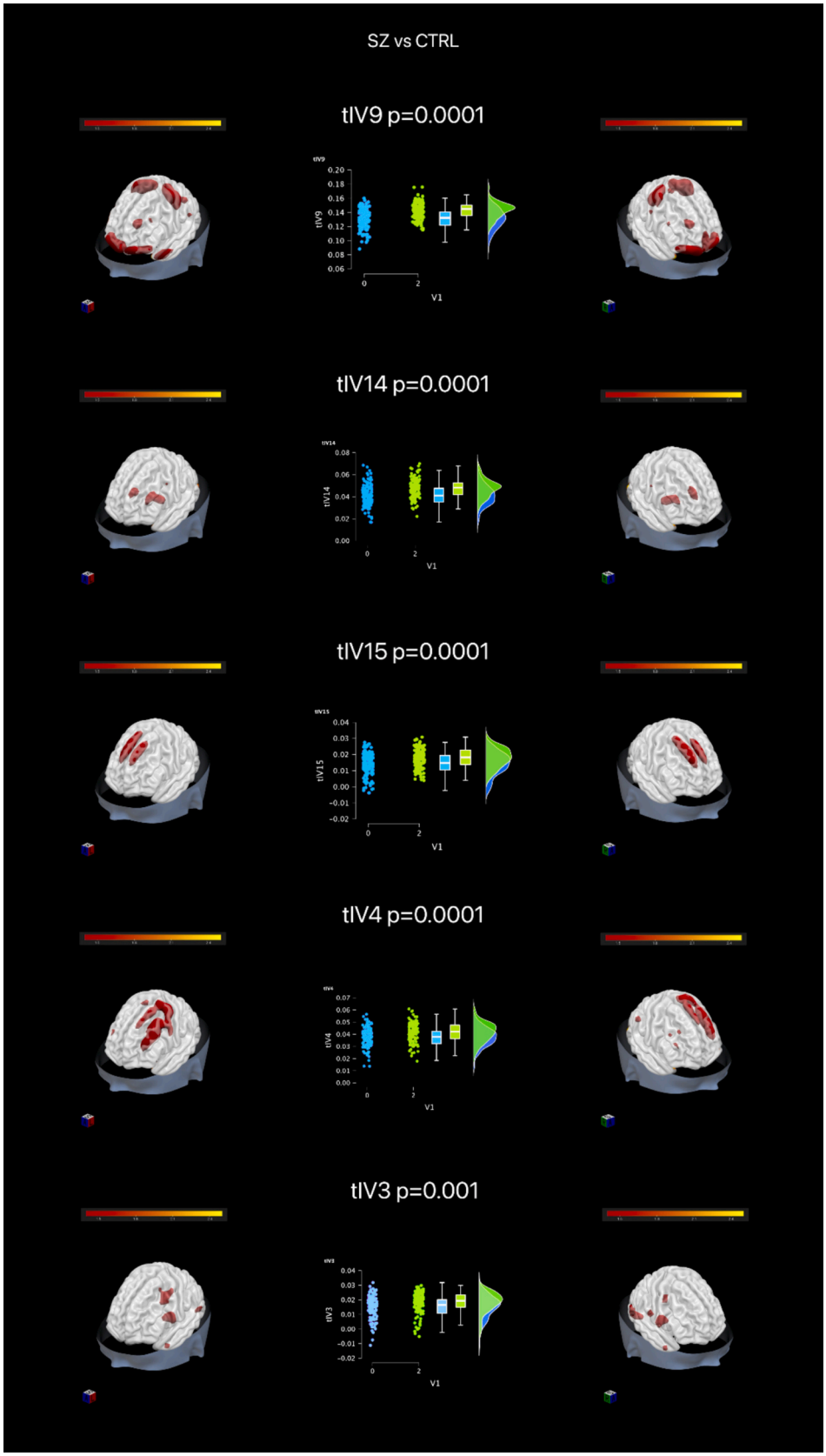

Fig. 4. Graphical representation of the white matter areas for the most significant networks, illustrating the t-test results for comparisons between Schizophrenic and Control patients.

Table 2
Table detailing important information of tIV14 network.

GM				
Area	Brodmann Area	volume (cc)	random effects: Max Value (x, y, z)	MNI (x, y, z)
Sub-Gyral	*	1.6/1.6	5.8 (−38, −68, 0)/7.3 (53, −45, −4)	(−38, −70, −4)/(54, −46, −8)
Middle Temporal Gyrus	19, 20, 21, 37, 39	5.4/4.0	6.6 (−57, −41, −1)/6.8 (53, −45, −8)	(−58, −42, −4)/(54, −46, −12)
Middle Occipital Gyrus	18, 19	3.9/4.0	6.6 (−42, −76, 0)/5.6 (42, −72, 4)	(−42, −78, −4)/(42, −74, 0)
Middle Frontal Gyrus	10, 11	1.2/0.8	6.5 (−26, 52, −9)/5.7 (34, 52, −9)	(−26, 54, −8)/(34, 54, −8)
Inferior Occipital Gyrus	18, 19	1.7/1.2	6.2 (−38, −80, −3)/4.5 (38, −80, −3)	(−38, −82, −8)/(38, −82, −8)
Inferior Temporal Gyrus	20, 37	0.3/0.4	6.2 (−38, −72, 0)/5.2 (53, −45, −11)	(−38, −74, −4)/(54, −46, −16)
Superior Frontal Gyrus	10	0.8/0.7	5.6 (−22, 56, −10)/5.2 (22, 56, −13)	(−22, 58, −8)/(22, 58, −12)
Superior Temporal Gyrus	22, 38, 39, 42	1.7/1.3	5.2 (−46, −52, 10)/4.7 (46, −52, 17)	(−46, −54, 8)/(46, −54, 16)
Angular Gyrus	39	0.5/0.6	4.4 (−34, −58, 36)/4.8 (42, −66, 33)	(−34, −62, 36)/(42, −70, 32)
Cuneus	7, 17, 18	1.1/0.4	4.7 (−22, −95, −2)/4.2 (30, −82, 23)	(−22, −98, −8)/(30, −86, 20)
Lingual Gyrus	17, 18	1.7/0.3	4.6 (−22, −92, −6)/3.9 (26, −80, −6)	(−22, −94, −12)/(26, −82, −12)
Precuneus	39	0.3/0.1	4.5 (−34, −62, 36)/4.3 (42, −66, 36)	(−34, −66, 36)/(42, −70, 36)
Medial Frontal Gyrus	25	0.2/0.1	3.8 (−2, 17, −18)/4.0 (2, 17, −18)	(−2, 18, −20)/(2, 18, −20)
Supramarginal Gyrus	*	0.0/0.4	−999.0 (0,0,0)/ 3.9 (42, −51, 36)	(0, 0, 0)/(42, −54, 36)
WM				
Area	Brodmann Area	volume (cc)	random effects: Max Value (x, y, z)	MNI (x, y, z)
Lentiform Nucleus	*	0.8/1.0	5.4 (−26, −2, 7)/5.1 (26, −2, 7)	(−26, −2, 8)/(26, −2, 8)
Extra-Nuclear	*	1.1/0.4	4.8 (−30, −6, 4)/5.1 (30, −2, 4)	(−30, −6, 4)/(30, −2, 4)

Table 3
Table detailing important information of tIV15 network.

GM				
Area	Brodmann Area	volume (cc)	random effects: Max Value (x, y, z)	MNI (x, y, z)
Superior Frontal Gyrus	6, 8, 9, 10	12.2/ 15.7	12.2 (−6, 36, 50)/ 12.4 (6, 36, 50)	(−6, 34, 56)/ (6, 34, 56)
Medial Frontal Gyrus	6, 8, 9, 10	3.0/2.3	11.2 (−6, 47, 42)/ 11.8 (6, 47, 42)	(−6, 46, 48)/ (6, 46, 48)
*	*	0.1/0.9	4.1 (−6, 13, 66)/ 9.6 (2, 24, 54)	(−6, 10, 72)/ (2, 22, 60)
Middle Frontal Gyrus	6, 8, 9	1.3/4.7	5.6 (−22, 35, 42)/ 7.7 (22, 20, 54)	(−22, 34, 48)/(22, 18, 60)
Cingulate Gyrus	32	0.2/0.3	4.3 (−2, 23, 39)/ 5.3 (2, 23, 39)	(−2, 22, 44)/ (2, 22, 44)
WM				
Area	Brodmann Area	volume (cc)	random effects: Max Value (x, y, z)	MNI (x, y, z)
Medial Frontal Gyrus	6, 8, 9, 10, 32	4.4/5.1	14.3 (−10, 35, 42)/15.3 (10, 35, 42)	(−10, 34, 48)/(10, 34, 48)
Superior Frontal Gyrus	6, 8, 9, 10	9.0/12.4	12.8 (−10, 28, 47)/14.9 (10, 31, 46)	(−10, 26, 52)/(10, 30, 52)
Middle Frontal Gyrus	6, 8	0.1/1.2	4.3 (−18, 20, 54)/ 9.1 (18, 5, 59)	(−18, 18, 60)/(18, 2, 64)
Sub-Gyral	6, 8	0.4/0.4	5.8 (−18, 35, 42)/ 8.6 (18, 9, 55)	(−18, 34, 48)/(18, 6, 60)
Cuneus	17, 23, 30	0.4/0.5	4.6 (−14, −75, 11)/5.8 (18, −67, 11)	(−14, −78, 8)/(18, −70, 8)
Posterior Cingulate	30	0.0/0.3	−999.0 (0, 0, 0)/ 4.5 (18, −64, 11)	(0, 0, 0)/(18, −66, 8)

with different densities compared to healthy controls, as reported in Supplementary Table S1.

Having found some noteworthy differences in global network structure across the 3 groups, we moved the analysis to a deeper level, considering the local clustering coefficient (see Methods) for individual regions across the 3 groups. Specifically, we focused on node tIV9 as it belonged to the center of the network skeleton, and on nodes tIV14 and tIV15, of relevance from previous analysis. We focused on these three nodes (tIV9, tIV14, tIV15) for two main reasons. First, our statistical and network analyses indicated that these nodes (or independent components) showed the most substantial group differences. In particular, tIV9 emerged as a central node connecting multiple other brain networks, while tIV14 and tIV15 corresponded to components that significantly differentiated schizophrenia from bipolar disorder and controls.

Second, these three components align well with the key findings from Sorella et al. (2019), who proposed an 'expanded continuum hypothesis' of schizophrenia and bipolar disorder, emphasizing a shared "psychotic core" but also partially distinct cognitive and affective-related circuits. Precisely, tIV9 matches the frontotemporal network previously linked to shared psychotic features in both disorders, while tIV14 and tIV15 map onto the posterior-temporal and medial frontal systems, respectively—networks that Sorella et al. identified as distinctively altered in schizophrenia versus bipolar disorder. Results are appended at the end of Supplementary Table S1.

Interestingly, the local clustering coefficients for nodes tIV9 and tIV14 differentiated individuals with the schizophrenic disorder from healthy controls (p_{iTV9} = .0003, p_{iTV14} = .0001) and also from individuals with the bipolar disorder (p_{iTV9} = .0068, p_{iTV14} = .0001). These differences would remain statistically significant even if one applied a Bonferroni correction for multiple testing. Instead, tIV15 did not highlight any differences in terms of local clustering coefficient in comparisons between groups. These patterns indicate that the neural activity captured by iTV9 and iTV14 might be relevant for detecting altered neutral integration/segregation patterns in schizophrenic individuals, with potential repercussions for detecting novel interventions for therapeutic and biomarking interventions.

4. General discussion

Although the dichotomous classification of schizophrenia (SCZ) and bipolar disorder (BD) remains widely used, numerous findings have challenged this perspective, suggesting the existence of a continuum between these conditions (Moller, 2003; Sorella et al., 2019, see also Supplementary Fig. S3). This study explored the neural differences and overlaps within the framework of the expanded continuum hypothesis

Table 4
table detailing important information of tIV9 network.

GM				
Area	Brodmann Area	volume (cc)	random effects: Max Value (x, y, z)	MNI (x, y, z)
Superior Temporal Gyrus	22, 38, 42	5.4/0.4	6.0 (−42, 20, −21)/4.2 (46, 20, −25)	(−42, 22, −24)/(46, 22, −28)
*	*	0.4/0.6	5.1 (−42, 20, −18)/4.5 (26, 44, −19)	(−42, 22, −20)/(26, 46, −20)
Middle Temporal Gyrus	21	2.9/0.1	5.5 (−57, 1, −14)/4.0 (57, 5, −14)	(−58, 2, −16)/(58, 6, −16)
Inferior Frontal Gyrus	44, 45, 47	1.2/0.1	4.7 (−38, 17, −18)/3.6 (38, 20, −18)	(−38, 18, −20)/(38, 22, −20)
Fusiform Gyrus	19, 37	0.6/0.0	4.6 (−50, −61, −14)/−999.0 (0, 0, 0)	(−50, −62, −20)/(0, 0, 0)
Inferior Temporal Gyrus	21, 37	0.4/0.0	4.6 (−61, −3, −17)/−999.0 (0, 0, 0)	(−62, −2, −20)/(0, 0, 0)
Middle Frontal Gyrus	9, 10, 11	0.8/0.1	4.5 (−34, 38, 20)/3.9 (50, 15, 29)	(−34, 38, 24)/(50, 14, 32)
Rectal Gyrus	11	0.2/0.1	4.5 (−2, 47, −26)/3.8 (6, 47, −26)	(−2, 50, −28)/(6, 50, −28)
Transverse Temporal Gyrus	41, 42	0.5/0.0	4.4 (−61, −17, 12)/−999.0 (0, 0, 0)	(−62, −18, 12)/(0, 0, 0)
Middle Occipital Gyrus	37	0.2/0.0	4.3 (−50, −65, −10)/−999.0 (0, 0, 0)	(−50, −66, −16)/(0, 0, 0)
Declive	*	0.3/0.0	4.3 (−50, −53, −21)/−999.0 (0, 0, 0)	(−50, −54, −28)/(0, 0, 0)
Precentral Gyrus	6, 44	0.3/0.0	4.1 (−57, −2, 7)/−999.0 (0, 0, 0)	(−58, −2, 8)/(0, 0, 0)
Sub-Gyral	*	0.3/0.0	4.1 (−34, 38, 17)/−999.0 (0, 0, 0)	(−34, 38, 20)/(0, 0, 0)
Superior Frontal Gyrus	10, 11	0.0/0.4	−999.0 (0, 0, 0)/4.0 (18, 61, 19)	(0, 0, 0)/(18, 62, 24)
Postcentral Gyrus	40	0.2/0.0	3.8 (−61, −24, 16)/−999.0 (0, 0, 0)	(−62, −26, 16)/(0, 0, 0)
Tuber	*	0.2/0.0	3.7 (−50, −50, −24)/−999.0 (0, 0, 0)	(−50, −50, −32)/(0, 0, 0)
WM				
Area	Brodmann Area	volume (cc)	random effects: Max Value (x, y, z)	MNI (x, y, z)
Orbital Gyrus	11	0.1/0.4	5.5 (−10, 51, −19)/8.7 (10, 51, −19)	(−10, 54, −20)/(10, 54, −20)
Superior Frontal Gyrus	10, 11	2.1/2.9	7.0 (−26, 56, −13)/8.3 (10, 55, −20)	(−26, 58, −12)/(10, 58, −20)
Medial Frontal Gyrus	11	0.2/0.5	5.2 (−10, 56, −16)/8.2 (10, 56, −16)	(−10, 58, −16)/(10, 58, −16)
Precentral Gyrus	4, 6	1.9/3.5	4.7 (−34, −27, 49)/6.9 (34, −11, 59)	(−34, −30, 52)/(34, −14, 64)
Middle Frontal Gyrus	10, 11, 47	2.3/1.9	6.3 (−26, 56, −10)/6.8 (34, 52, −9)	(−26, 58, −8)/(34, 54, −8)
Sub-Gyral	*	1.7/0.6	5.1 (−10, −34, 61)/6.4 (14, 51, −19)	(−10, −38, 64)/(14, 54, −20)
Middle Temporal Gyrus	20, 21	1.2/0.1	6.0 (−46, 5, −24)/3.7 (57, −41, −11)	(−46, 6, −28)/(58, −42, −16)
Rectal Gyrus	11	0.0/0.2	−999.0 (0, 0, 0)/5.7 (10, 51, −23)	(0, 0, 0)/(10, 54, −24)
Superior Temporal Gyrus	38	1.1/0.1	5.7 (−42, 9, −24)/3.6 (42, 12, −28)	(−42, 10, −28)/(42, 14, −32)
Postcentral Gyrus	2, 3, 4, 40, 43	2.3/0.8	5.2 (−38, −30, 53)/4.2 (42, −23, 49)	(−38, −34, 56)/(42, −26, 52)
Precuneus	*	0.3/0.0	5.0 (−26, −58, 40)/−999.0 (0, 0, 0)	(−26, −62, 40)/(0, 0, 0)
Paracentral Lobule	4	0.4/0.0	4.9 (−14, −34, 57)/−999.0 (0, 0, 0)	(−14, −38, 60)/(0, 0, 0)
Thalamus	*	0.0/0.2	−999.0 (0, 0, 0)/4.4 (10, −21, 5)	(0, 0, 0)/(10, −22, 4)
Extra-Nuclear	*	0.2/0.1	4.2 (−2, 18, 14)/3.7 (2,22,10)	(−2, 18, 16)/(2,22,12)
*	*	0.1/0.2	3.7 (−42, 36, −15)/4.2 (2, 18, 14)	(−42, 38, −16)/(2, 18, 16)

(Sorella et al., 2019, see Supplementary Fig. S3), by relying on a data fusion machine learning approach known as tIVA. Gray and White matter images of 128 individuals with schizophrenia (SZ), 128 with bipolar disorder (BD), and 127 healthy controls (CTRL), matched for gender, age, and IQ were taken into consideration. Results confirmed both a common neural substrate (tIV9) and differences (tIV14 and tIV15). Moreover, the SZ group displayed the highest degree of compromission compared to CTRL (three additional networks altered: tIV3,4,11). The BD group occupied an intermediate position on this continuum, with fewer abnormalities than SZ but more than CTRL. Further network analysis revealed significant differences in clustering coefficient and density in SZ compared to controls, whereas BD showed no substantial differences from CTRL.

Collectively, these findings lend neurobiological support to the expanded continuum hypothesis, suggesting that SZ and BD may represent different points on a shared spectrum of neuroanatomical alterations. This dimensional perspective is increasingly vital for understanding the complex overlap between SZ and BD, and it is corroborated by evidence from various domains. Complementary support for such a transdiagnostic, dimensional approach comes from studies examining other neurobiological markers and clinical features linked to underlying brain function. For instance, Magioncalda et al. (2020) investigated intrinsic functional brain activity related to psychomotor alterations, a core feature in both SZ and BD. They found that specific patterns of functional connectivity within the subcortical-cortical sensorimotor system, particularly involving thalamus-sensorimotor network coupling and its modulation by substantia nigra and raphe nuclei pathways, were associated with psychomotor inhibition or excitation, irrespective of whether the patient was diagnosed with SZ or BD. These findings, demonstrating that neural correlates of specific symptom dimensions can cut across traditional diagnostic boundaries, resonate strongly with our identification of covarying structural gray and white matter networks that place SZ and BD on a spectrum. Indeed, the structural network abnormalities we identified may represent the anatomical substrate upon which such symptom-specific functional disconnections, as reported by Martino and colleagues, manifest. For example, compromised structural integrity in networks like our shared fronto-temporal tIV9, or the graded alterations in other networks (tIV3, tIV4, tIV14, tIV15), could impair their capacity for efficient information

Table 5
table detailing important information of tIV4 network.

GM				
Area	Brodmann Area	volume (cc)	random effects: Max Value (x, y, z)	MNI (x, y, z)
Middle Frontal Gyrus	6, 8, 9, 10, 46	19.7/3.1	10.2 (−42, 20, 43)/ 6.4 (50, 34, 20)	(−42, 18, 48)/(50, 34, 24)
Precentral Gyrus	4, 6, 9	3.9/0.1	9.1 (−46, 19, 36)/ 3.5 (46, 23, 36)	(−46, 18, 40)/(46, 22, 40)
Superior Frontal Gyrus	6, 8, 9, 10	12.1/0.0	9.0 (−34, 20, 51)/ −999.0 (0, 0, 0)	(−34, 18, 56)/(0, 0, 0)
Inferior Frontal Gyrus	9, 45, 46	2.9/0.7	7.9 (−50, 11, 33)/ 4.7 (53, 26, 21)	(−50, 10, 36)/(54, 26, 24)
Medial Frontal Gyrus	6	0.1/0.0	5.2 (−14, 5, 62)/ −999.0 (0, 0, 0)	(−14, 2, 68)/(0, 0, 0)
Sub-Gyral	6	0.3/0.0	5.0 (−26, −3, 55)/ −999.0 (0, 0, 0)	(−26, −6, 60)/(0, 0, 0)
Postcentral Gyrus	3	0.3/0.0	4.7 (−50, −11, 48)/−999.0 (0, 0, 0)	(−50, −14, 52)/(0, 0, 0)
WM				
Area	Brodmann Area	volume (cc)	random effects: Max Value (x, y, z)	MNI (x, y, z)
Middle Frontal Gyrus	6, 8, 9, 10, 46	11.5/1.6	11.3 (−34, 19, 40)/ 6.5 (38, 38, 20)	(−34, 18, 44)/(38, 38, 24)
Precentral Gyrus	4, 6, 9	6.3/0.0	9.7 (−38, 19, 36)/ −999.0 (0, 0, 0)	(−38, 18, 40)/(0, 0, 0)
Sub-Gyral	6	2.2/0.2	8.6 (−34, 34, 20)/ 3.9 (34, 38, 17)	(−34, 34, 24)/(34, 38, 20)
Superior Frontal Gyrus	6, 8, 9	5.1/0.0	7.6 (−18, −10, 63)/−999.0 (0, 0, 0)	(−18, −14, 68)/(0, 0, 0)
Medial Frontal Gyrus	6, 8	1.8/0.0	6.5 (−10, 5, 59)/ −999.0 (0, 0, 0)	(−10, 2, 64)/(0, 0, 0)
Thalamus	*	1.4/1.0	5.6 (−10,−13,12)/ 5.4 (10,−13,12)	(−10, −14, 12)/(10, −14, 12)
Inferior Parietal Lobule	40	0.0/1.0	−999.0 (0, 0, 0)/ 4.9 (46, −50, 39)	(0, 0, 0)/ (46, −54, 40)
Supramarginal Gyrus	40	0.0/0.8	−999.0 (0, 0, 0)/ 4.8 (46, −51, 36)	(0, 0, 0)/ (46, −54, 36)
Middle Temporal Gyrus	39	0.0/0.3	−999.0 (0, 0, 0)/ 4.6 (42, −63, 29)	(0, 0, 0)/ (42, −66, 28)
Inferior Frontal Gyrus	9	0.2/0.0	4.3 (−53, 7, 29)/ −999.0 (0, 0, 0)	(−54, 6, 32)/(0, 0, 0)
Lingual Gyrus	17	0.3/0.0	4.1 (−22, −95, −5)/−999.0 (0, 0, 0)	(−22, −98, −12)/(0, 0, 0)
Angular Gyrus	*	0.0/0.2	−999.0 (0, 0, 0)/ 4.1 (42, −66, 33)	(0, 0, 0)/ (42, −70, 32)

Table 6
table detailing important information of tIV3 network.

GM				
Area	Brodmann Area	volume (cc)	random effects: Max Value (x, y, z)	MNI (x, y, z)
Pyramis	*	4.0/3.7	13.8 (−18, −73, −30)/14.1 (22, −73, −30)	(−18, −74, −40)/(22, −74, −40)
Uvula	*	2.4/2.2	11.9 (−18, −74, −33)/12.2 (14, −77, −26)	(−18, −74, −44)/(14, −78, −36)
Cerebellar Tonsil	*	3.8/4.0	11.0 (−30, −66, −34)/11.6 (30, −66, −34)	(−30, −66, −44)/(30, −66, −44)
Tuber	*	1.5/2.0	9.6 (−30, −66, −30)/10.8 (30, −69, −30)	(−30, −66, −40)/(30, −70, −40)
Inferior Semi-Lunar Lobule	*	1.9/2.4	9.6 (−30, −66, −37)/10.4 (34, −66, −37)	(−30, −66, −48)/(34, −66, −48)
Declive	*	0.4/0.6	4.4 (−14, −73, −20)/4.9 (18, −73, −20)	(−14, −74, −28)/(18, −74, −28)
*	*	0.2/0.1	4.1 (−18, −65, −24)/3.6 (18, −65, −24)	(−18, −66, −32)/(18, −66, −32)
WM				
Area	Brodmann Area	volume (cc)	random effects: Max Value (x, y, z)	MNI (x, y, z)
Culmen	*	0.4/0.6	4.7 (−2, −53, −14)/4.8 (2, −53, −14)	(−2, −54, −20)/(2, −54, −20)
Cerebellar Lingual	*	0.1/0.1	4.1 (−6, −49, −18)/4.5 (6, −49, −18)	(−6, −50, −24)/(6, −50, −24)
Inferior Occipital Gyrus	*	0.0/0.3	−999.0 (0, 0, 0)/ 4.3 (34, −72, −3)	(0, 0, 0)/(34, −74, −8)

processing and dynamic functional coupling. This, in turn, might make individuals more vulnerable to the types of functional dysconnectivity within sensorimotor and modulatory circuits observed during specific psychomotor states. Conversely, it is also conceivable that chronic functional dysregulation contributes to the observed structural covariance patterns. In either case, both our structural perspective and their functional investigations converge to support a dimensional model where underlying structural predispositions and more dynamic, symptom-related functional alterations interact, contributing to the varied clinical presentations along the SZ-BD spectrum. Together, such studies underscore the utility of an RDoC-like approach, moving beyond categorical classifications to explore underlying dimensional pathophysiological processes.

Our approach, focusing on identifying covarying gray and white matter networks, aligns with a growing body of research demonstrating that mapping intrinsic brain connectivity networks offers a robust and potentially mechanistic framework for understanding complex aspects of human behavior and mental disorders. Rather than viewing pathologies as isolated to specific brain regions, network-based approaches can unify heterogeneous neuroimaging findings and reveal how distributed alterations contribute to symptomatology. For instance, recent studies leveraging network localization have provided significant insights into the neural mechanisms underlying specific symptoms like auditory verbal hallucinations (Mo et al., 2024), broader psychiatric phenomena such as suicide risk (Zhang et al., 2024), and the interplay between structural atrophy and cognitive dysfunctions in schizophrenia (Cheng et al., 2025). Furthermore, such network perspectives can elucidate how brain abnormalities evolve across different stages of a disorder, as shown in schizophrenia (Xu et al., 2024), thereby offering refined neuropathological models and potential targets for intervention. The tIVA networks identified in our study can be interpreted within this context, representing interconnected systems whose disruptions contribute to the shared and distinct features of SZ and BD along a continuum.

It is important to consider how the structural covarying gray and white matter networks identified in our study relate to the vast body of

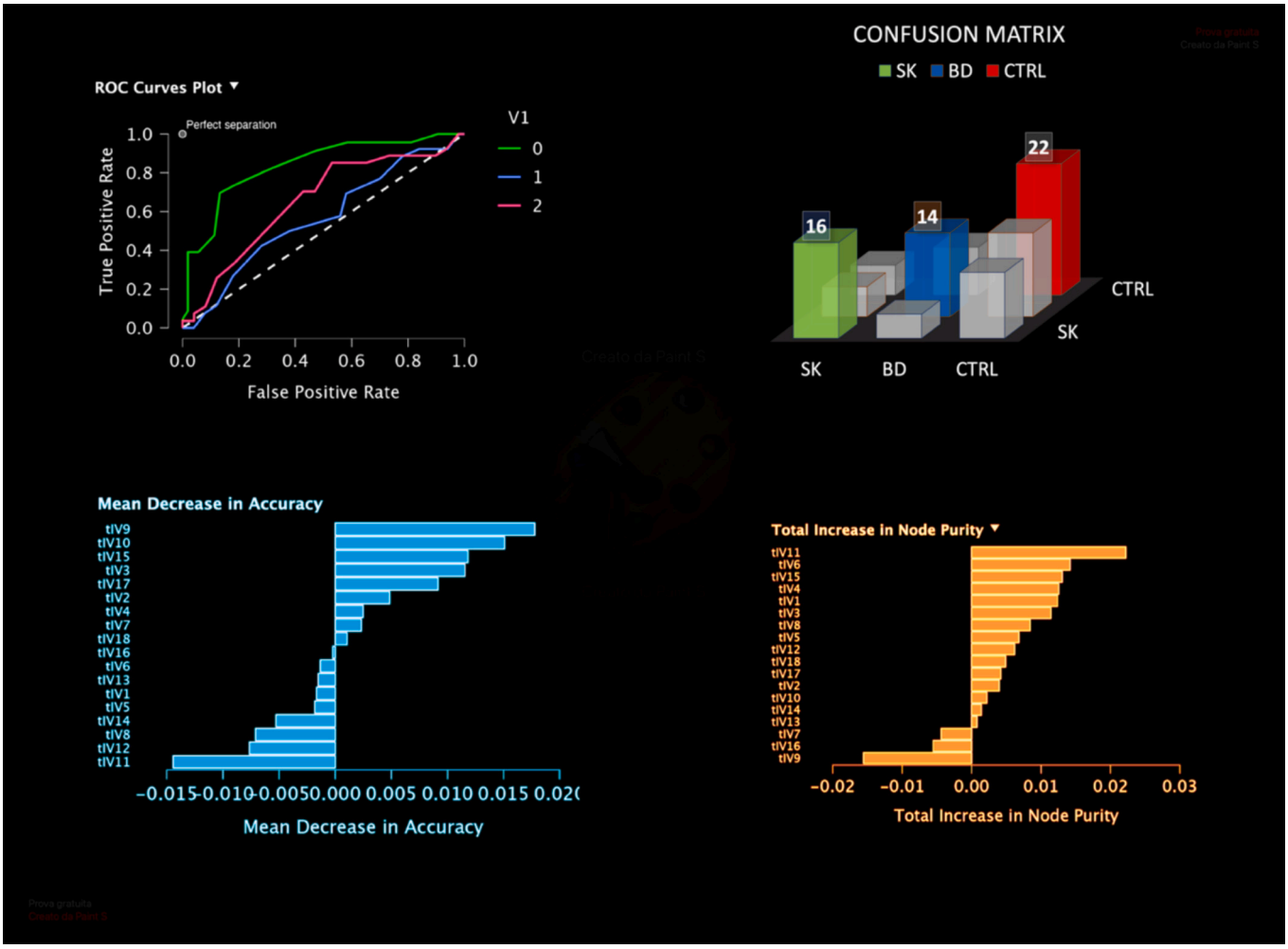

Fig. 5. Plots showcasing the ROC curves for model classifications, the out-of-bag accuracy, the mean decrease in accuracy, the node purity, and the confusion matrix (in 5).

literature on functional connectivity abnormalities in schizophrenia (SZ) and bipolar disorder (BD). Structural connectivity, such as white matter pathways and the coordinated variation of gray matter regions, is generally considered to provide the anatomical backbone that shapes, constrains, and facilitates functional interactions between brain regions (Honey et al., 2009; van den Heuvel and Sporns, 2013). Therefore, the alterations we observed in specific tIVA networks, representing atypical patterns of gray and white matter co-variance, likely have significant implications for functional brain dynamics.

For example, the shared fronto-temporal network (tIV9) that showed reduced matter concentration in both SZ and BD patients compared to controls, and particularly in SZ, is composed of regions critical for emotional processing, reality testing, and higher-level cognitive integration. Structural deficits in this network could plausibly lead to dysregulated functional connectivity within fronto-temporal circuits. Such functional dysconnectivity has been frequently reported in both SZ and BD and is thought to underlie core psychotic symptoms and affective disturbances (Garrity et al., 2007; Meda et al., 2012; Dong et al., 2018). Similarly, the distinct networks that differentiated SZ from BD (e.g., tIV14, tIV15 involving posterior-temporal/occipital and medial frontal regions, respectively) may point to structural vulnerabilities that predispose to specific patterns of functional dysconnectivity underlying the differential cognitive and affective symptom profiles of these disorders. For instance, alterations in medial frontal networks (tIV15) in SZ could underpin disruptions in functional networks crucial for executive functions and self-monitoring, often found to be compromised in this condition (Minzenberg et al., 2009).

While our current study did not directly assess functional connectivity, the identified structural networks provide a valuable map of potential sites of functional disruption. Future research integrating multimodal imaging by examining functional connectivity within and between these structurally defined tIVA networks would be crucial for a more comprehensive understanding of the complex interplay between brain structure and function in the pathophysiology of SZ and BD along the proposed continuum.

These combined neurobiological and conceptual insights provide a strong foundation for the detailed discussion of our specific network findings that follow. In the next sections, we discuss these results in detail.

4.1. *A shared fronto-temporal networks in SZ and BD (tIV9)*

Our analyses demonstrated a shared fronto-temporal network altered in SZ and BD patients compared to controls. The tIV9 network was our main shared network encompassing this fronto-temporal network; it primarily comprises frontal (inferior/superior frontal gyri) and temporal (superior, middle, inferior, and transverse temporal gyri) areas, along with the fusiform gyrus and adjacent white matter. As discussed by Sorella et al. (2019), neuropsychological research indicates that damage to regions, including posterior temporo-parietal areas and fronto-temporo-parietal regions, particularly within the right hemisphere can lead to psychotic symptoms, including multimodal

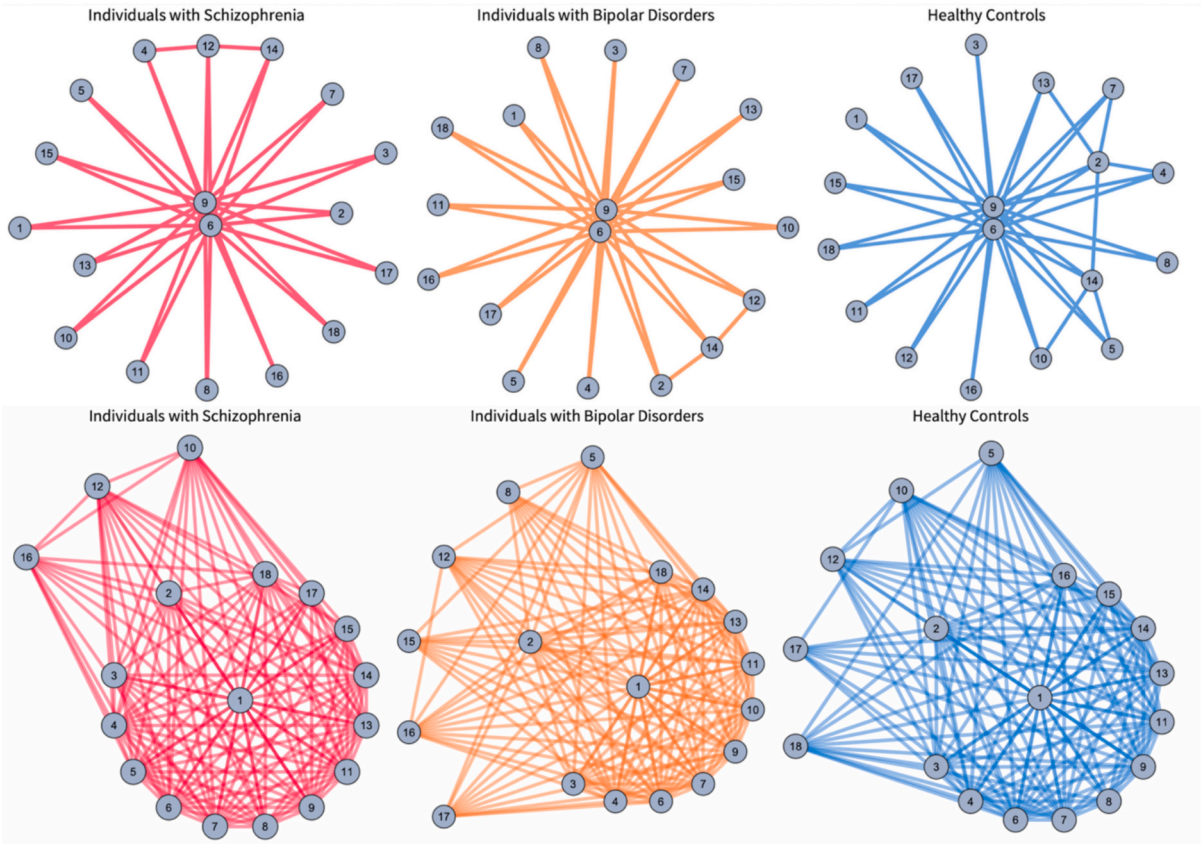

Fig. 6. Network visualizations computed across different groups using Wolfram Mathematica, with the top figure illustrating the threshold $T = 0.07$ and the bottom figure showing the threshold $T = 0.03$. Links are included if at least one individual shows differences in activation levels. Most subjects exhibit a similar pattern at T = 0.07, particularly at nodes 6 and 9, which display activation levels markedly different from other brain regions. The visualizations are plotted using a radial layout to effectively illustrate these differences, with the lower threshold of T = 0.03 highlighting more nuanced contrasts.

hallucinations (Rabins et al., 1991; Kumral and Ozturk, 2004; Bielawski and Bondurant, 2015; Stangeland et al., 2018; Ffytche and Wible, 2014). More specifically, abnormalities in the ventro-temporo-occipital area observed in SZ and BD (Lochhead et al., 2004; McDonald et al., 2000) may contribute to the visual processing impairments that are characteristic of both disorders (Doniger et al., 2002; Butler et al., 2008; Fernandes et al., 2017), thereby disrupting the information necessary for accurate real-world perception (Ffytche and Wible, 2014; Logothetis et al., 1995). Thus, disruptions in ventrotemporal and medial parieto-occipital areas, as well as portions of the cerebellum and the middle frontal gyrus regions, could represent a common neural substrate in SZ and BD. Potentially reflecting an altered "psychotic core" that affects reality testing, emotion perception, and higher-level integrative processes in both schizophrenic (see also Kaspárek et al., 2010; Gupta et al., 2015; Laidi et al., 2015) and bipolar patients (Lochhead et al., 2004; Rimol et al., 2010).

Abnormalities in the temporal cortex have long been associated with perceptual distortions and psychotic symptoms. As reviewed by Sorella et al. (2019), structural and functional disruptions in middle/inferior temporal and transverse temporal regions can interfere with one's capacity to integrate and interpret sensory information (e.g., auditory or visual stimuli), thereby contributing to hallucinations or delusional thinking in both SZ and BD (Doniger et al., 2002; Butler et al., 2008; O'Bryan et al., 2014; Fernandes et al., 2017). Grecucci et al. (2023) found that the temporal lobe, including the fusiform, the parahippocampal gyrus, and the temporal gyrus, was hyperactivated in SZ subjects when compared to BD during negative visual stimulus processing, implying that shared dysfunctions here may amplify negative emotional reactivity. Beyond the significance of emotional processes of the left superior temporal gyrus and the left fusiform gyrus (Vytal and Hamann, 2010), the left superior temporal gyrus has been associated with severe auditory verbal hallucinations in SCZ (Modinos et al., 2013). In addition, some evidence indicates that the uncus may be implicated in hallucinations (Fortuna et al., 2001; Roberts et al., 2001). The left parahippocampal region also appears to play a role, as its deactivation has been linked to auditory verbal hallucinations in SCZ (Diederen et al., 2010). The fusiform gyrus is traditionally implicated in face/object recognition but also in the nuanced evaluation of emotional stimuli (Rimol et al., 2010 for SZ). Its disruption can lead to misinterpretations of social and affective cues, which Doniger et al. (2002) and Fernandes et al. (2017) link to both disorders' propensity for perceptual anomalies and heightened emotional reactivity. The frontal gyrus plays vital roles in executive functions, emotion regulation, and top-down cognitive control. A meta-analysis focused on response inhibition revealed atypical activation in the right inferior frontal gyrus (IFG) and right middle frontal gyrus (MFG) among BD patients (Hajek et al., 2013; see also Stefanopoulou et al., 2009). Notably, this impaired response inhibition has been proposed as the most prominent cognitive endophenotype of bipolar disorder (Bora et al., 2009; Lapomarda et al., 2021a, 2021b).

Included in tIV9 are white matter regions adjacent to fronto-temporal areas, consistent with the view that dysconnectivity in these pathways impedes seamless communication between emotional-limbic and executive regions. Other studies have already demonstrated that white matter tracts adjacent to these areas can be compromised in BD and SZ patients or both (Heng et al., 2010; McIntosh et al., 2008; Sussmann et al., 2009; Samartzis et al., 2014). Overall, these tIV9 findings echo the expanded continuum hypothesis (Sorella et al., 2019), wherein SZ and BD share fronto-temporal circuit disruptions relevant to psychotic manifestations (altered perception, salience misattribution) yet differ in additional networks. By affecting the superior, middle, and

inferior temporal gyri, transverse temporal cortex, fusiform gyrus, inferior/superior frontal gyri, and their white matter connections, tIV9 likely anchors crucial deficits in emotional perception and cognitive integration. In this way, it underscores a "common ground" in SZ and BD pathophysiology, lending neurobiological support to the notion that these disorders partially overlap in their psychotic or affective underpinnings (Sorella et al., 2019; Grecucci et al., 2023).

4.2. Distinct networks in SZ and BD (tIV14- tIV15)

In our analyses, tIV14 and tIV15 differentiated significantly between SZ and BD patients. tIV14 encompasses posterior temporal regions, occipital areas (including the cuneus), the precuneus, and subgyral spaces. While Sorella et al. (2019) primarily highlighted a "psychotic core" shared by schizophrenia and bipolar disorder in more ventral and frontal-temporal circuits, they also reported partial evidence of specific gray matter alterations in certain regions for individuals with BD compared to individuals with SZ, suggesting that other cortical changes could differentiate these two disorders. Indeed, they note that at a more liberal threshold, SZ showed more pronounced reductions than BD in regions such as cerebellar, temporal, and occipital areas. The specific regions comprehended the lingual gyrus, the superior and the inferior parietal lobule, the precuneus and other parieto occipial areas. They also note that BD showed more pronounced reductions at a higher threshold than SZ in occipital and other areas such as occipital gyrus, cuneus, and precuneus. The emerging picture was that BD may involve additional or distinct abnormalities that link to affect-driven processes and mood dysregulation (Sorella et al., 2019). The dysfunction observed in the ventro-temporo-occipital region in individuals with SZ and BD (Lochhead et al., 2004; McDonald et al., 2000) may contribute to the visual processing deficits that are commonly associated with both conditions (Doniger et al., 2002; Butler et al., 2008; O'Bryan et al., 2014; Fernandes et al., 2017). The cuneus is implicated in visuospatial aspects of emotion and negative stimulus processing, while the precuneus and the posterior cingulate cortex play a significant role in self-reflection among individuals with SZ (Meer et al., 2012), as well as in internal cognition and cognitive insight (Leech and Sharp, 2013; Zhang et al., 2015). A further distinction for tIV14 may concern subgyral involvement in the temporal and occipital lobes, which can reflect subtle white matter disruptions beneath cortical areas responsible for visual association and complex perceptual integration as discussed by Mahon et al., 2010.

tIV14 network also comprehends white matter regions, such as the Lentiform nucleus and white matter adjacent to the basal ganglia. Grecucci et al., 2023 also found these areas to be altered in BD and SZ patients. Other studies suggest the presence of structural anomalies in the basal ganglia during early-stage BD (Strakowski et al., 2005) and shape abnormalities in BD (Hwang et al., 2006). Likewise, SCZ patients exhibit altered basal ganglia volume and shape (Hirjak et al., 2015; Mamah et al., 2007; van Erp et al., 2016). Dysregulation of dopaminergic neurons in the basal ganglia (Haber, 2014) appears to induce an excessive attribution of salience to neutral stimuli (see the review by Howes and Kapur, 2009), which plays a pivotal role in the psychotic manifestations of both disorders (for reviews, see Kapur, 2003; Seeman and Kapur, 2000; Strakowski, 2014; Toda and Abi-Dargham, 2007). Notably, Li et al., 2021, add to the growing body of evidence that the lentiform nucleus is integral not only to motor functions but also to higher-order cognitive processes in schizophrenia. The study showed an increase in LN activity (fALFF) for SZ; its positive correlation with working memory and processing speed tests suggests that LN dysfunction is part of the broader neural circuitry underlying cognitive deficits in schizophrenia. Taken together, these indications from Sorella et al., 2019, and Grecucci et al., 2023, suggest that tIV14 encompassing subgyral areas, posterior temporal regions, occipital cortex (cuneus), and the precuneus may underlie distinct alterations linked to the mood-driven and perceptual-affective disruptions seen in BD. Although SZ can show abnormalities in similar brain regions, the emphasis on posterior cortical deficits might be more pronounced or functionally relevant in BD, potentially aligning with a more affective-laden presentation in this disorder. Consequently, while SZ and BD share overarching psychotic vulnerabilities, tIV14 highlights one way in which the disorders diverge, reinforcing the notion of an "expanded continuum" wherein BD's posterior temporal–occipital networks figure more prominently in its affective symptomatology, and SZ exhibits more significant dysfunction elsewhere (Sorella et al., 2019; Grecucci et al., 2023).

In our analyses, tIV15 centers primarily on the medial frontal gyrus and the cingulate cortex, along with white matter adjacent to these regions. Sorella et al., 2019, also indicated abnormalities of the medial frontal gyrus when comparing patients with schizophrenia with patients with bipolar disorder. In their study, the medial frontal gyrus appears in a component that was more reduced in SZ subjects relative to BD. Extensive fronto-parietal gray matter loss in schizophrenic patients is frequently documented in the literature (Minzenberg et al., 2009; Repovš and Barch, 2012), potentially reflecting the heightened severity of cognitive impairment, encompassing executive function, verbal memory, fluency, and working memory observed in this population (Krabbendam et al., 2005; Selva et al., 2007; Bora and Pantelis, 2015; Bortolato et al., 2015). Notably, cognitive impairment has been put forward as a potential differentiating factor between SZ and BD in categorical diagnoses, mainly due to the more pronounced memory deficits observed in the former (Rheenen et al., 2016). This aligns with the notion that schizophrenia often shows broader fronto-parietal or fronto-medial deficits affecting cognitive and executive functions, an area Sorella et al. (2019) termed the "cognitive core." Additionally, comparative studies of SZ and BD have highlighted the cingulate gyrus, especially in the posterior cingulate. Sorella et al. (2019) found that the posterior cingulate was part of an independent component that showed volume reduction in both SZ and BD patients relative to healthy controls.

As discussed before, together with the precuneus, the posterior cingulate cortex plays a significant role in self-reflection among individuals with SZ (Meer et al., 2012), as well as in internal cognition and cognitive insight (Leech and Sharp, 2013; Zhang et al., 2015). Notably, Grecucci et al. (2023) have provided further evidence of structural alterations in these same regions (including cingulate and basal ganglia). Their findings support the role of fronto-limbic and basal ganglia dysfunction in both disorders, specifically concerning reward processing, affective regulation, and salience attribution, but suggest that unique patterns of structural and functional abnormalities can be used to differentiate the two diagnostic groups. In particular, the basal ganglia and thalamus, which are both key components of the reward circuit and crucial for emotional processing (Haber and Knutson, 2010; Lapomarda et al., 2021a, 2021b), are implicated in abnormal responses to negatively valenced stimuli in both SZ and BD.

White matter adjacent to the frontal gyrus and the cingulate is also present in our tIV15 network. Previous studies indicated abnormalities in white matter tracts of the cingulate in BD subjects (Benedetti et al., 2011; Mahon et al., 2010), while Kanaan et al., 2009; did not find the Cingulate white matter traits to be affected in SZ subjects. This could also indicate a distinction between the two conditions based on this region or network including this region. These convergent lines of evidence thus point to shared but distinct neuroanatomical and neurofunctional alterations in SZ and BD, particularly within the cingulate cortex, medial frontal regions, and basal ganglia, that may underlie the greater severity of cognitive deficits in schizophrenia while also offering potential markers to differentiate it from bipolar disorder.

4.3. Specific networks for SZ (tIV3–4)

Two components, tIV3 and tIV4, emerged from our analyses as particularly relevant for distinguishing SZ from control subjects. tIV3 involved the cerebellum in gray matter (GM) and white matter (WM).

Sorella et al. (2019) highlighted a common psychotic substrate shared by the two disorders while reporting evidence of more extensive or differentially localized abnormalities. In Sorella et al., 2019 analyses, the cerebellum emerges in both a shared network across SZ and BD and in two networks that differentiate them, where BD shows more pronounced gray matter reductions. One component encompassing portions of the cerebellum was reduced in both SZ and BD patients relative to controls, consistent with the idea of an overlapping or "psychotic" core. Two other components involving the cerebellum were reduced specifically in BD relative to SZ. Grecucci et al. (2023) likewise found distinct alterations in subcortical and cerebellar structures tied to affective and perceptual processes. In particular, they found a cluster located in the left Cerebrum and left cerebellum, including the limbic lobe, the temporal lobe, and the anterior lobe. As discussed before, brain damage in a variety of regions, including the cerebellum, could produce psychotic symptoms (Rabins et al., 1991; Kumral and Ozturk, 2004; Bielawski and Bondurant, 2015; Stangeland et al., 2018), and these areas have been found to exhibit structural abnormalities in both SZ (Kaspárek et al., 2010; Gupta et al., 2015; Laidi et al., 2015) and BD (Lochhead et al., 2004; Rimol et al., 2010) subjects. Sorella et al., 2019 suggested that the cerebellum is part of the shared psychotic core that is common in both SZ and BD. However, they also argue that the cerebellum could singularly differentiate the two conditions.

Regarding white matter alteration of the cerebellum, Koch et al., 2010, investigated white matter (WM) integrity in subacute schizophrenia and identified widespread fractional anisotropy (FA) reductions in cortical and subcortical tracts, notably corticopontine-cerebellar projections. They proposed that disrupting this "cerebro-ponto-cerebellar loop," commonly essential for smooth-pursuit eye movements, motor coordination, and likely cognitive integration, could help explain motor deficits, "neurological soft signs," and psychotic manifestations often observed in SZ. Kim et al., 2021, similarly reported decreased FA in the middle cerebellar peduncle (MCP) among SZ patients, correlating inversely with executive function tasks (e.g., TMT—B, WCST). They interpreted these data through "cognitive dysmetria," suggesting that an impaired cerebellum struggles to provide corrective feedback to the cerebrum, thus impeding goal-directed cognition and intensifying the cognitive dysfunction characterizing SZ. Both studies underscore that white matter dysconnectivity in the cerebellum may not only disrupt motor coordination but also undermine higher-order cognitive processes central to schizophrenia's symptomatology.

Our tIV4 network comprises middle frontal, precentral, superior, and inferior frontal gyri in gray matter, as well as white matter adjacent to the middle, superior, and medial frontal gyri, precentral gyrus, sub-gyral regions, and the thalamus. Together, these areas form a fronto-temporal and fronto-thalamic circuit often implicated in the broader cognitive and executive dysfunctions characteristic of schizophrenia. While Sorella et al. (2019) outlined a shared "psychotic core" that can involve frontal and temporal pathways in both SZ and bipolar disorder (BD), they also emphasized that fronto-medial and fronto-parietal impairments are often more extensive in SZ, mirroring the more pronounced cognitive deficits and disorganized thinking observed in this condition.

Other work has detailed the white matter disruptions that may underlie these anatomical findings. For instance, Samartzis et al. (2014) stress the consistent presence of subtle and widespread WM deficits early in schizophrenia, particularly in fronto-temporal and fronto-limbic tracts that govern higher-order integration. This aligns well with tIV4's inclusion of the frontal gyrus (inferior, middle, and superior segments) and thalamic regions, suggesting a link between impaired WM integrity here and SZ patients' cognitive fragmentation and psychotic manifestations.

Studies of ventricular enlargement and regional gray/white matter changes, such as Horga et al., 2011, reinforce the notion that thalamic volume reductions and adjacent WM disturbances often accompany schizophrenic pathology. Although they did not pinpoint a strict local "compression" effect, the data consistently revealed that thalamic and periventricular white matter abnormalities correlated with cortical loss and, in some cases, with symptom severity. These disruptions likely impact executive, affective, and perceptual domains central to SZ, aligning with the broader deficits captured by tIV4. Thus, while Sorella et al. (2019) and Grecucci et al. (2023) detail gray matter alterations in frontal-thalamic regions for SZ, the evidence from Samartzis et al., 2014 clarifies how white matter dysconnectivity in these same circuits can intensify cognitive disorganization and psychotic symptoms. In line with tIV4's structure, frontal WM pathways connecting to the thalamus, already implicated in attentional control and sensory gating, would be especially vulnerable, distinguishing SZ from controls by undermining the seamless communication essential for coherent information processing.

Beyond the specific cortico-centric patterns that emerged as most differentiating between groups in our tIVA networks, it is crucial to consider the broader pathophysiological role of subcortical structures in schizophrenia (SZ) and bipolar disorder (BD). While our study did not identify primarily subcortical gray matter networks that robustly separated all three groups based on volumetric analysis, subcortical systems, especially those involved in neurotransmission, are fundamental in modulating the large-scale cortical networks where we did observe alterations. Conio et al. (2020) provide a comprehensive review of how dopaminergic and serotonergic systems, with key nuclei located subcortically (e.g., substantia nigra/ventral tegmental area and raphe nuclei, respectively), exert significant and often contrasting influences on resting-state networks implicated in these disorders. For example, dysregulation in the dopamine system, heavily involving basal ganglia circuits, is a cornerstone of psychosis theories relevant to both SZ and aspects of BD. Similarly, serotonergic pathways modulate mood and cognitive functions often disturbed in these conditions. It is, therefore, plausible that alterations in these subcortical modulatory systems contribute to the development or expression of the cortically-weighted structural covariance patterns captured by our tIVA networks, reflecting a complex interplay between subcortical neurochemistry and large-scale network organization along the SZ-BD continuum (See.

4.4. Network organization in SZ and BD

Our findings indicate that the network approach can find structural differences in the activation levels of different regions across groups of healthy individuals (CTRL), individuals with schizophrenia (SZ), and people with bipolar disorder (BD). Importantly, our analysis shows that these structural differences can depend in their directionality according to the threshold used for building the network structure. For instance, with one threshold, networks from the SZ group exhibited a higher median of clustering coefficient compared to the controls, whereas with another threshold, it was the controls' networks that were more clustered – in median – than networks from the SZ group. Because of these issues with the thresholding approach, one should: (i) focus on structural differences that persist across threshold and (ii) focus on statistical tests, possibly losing the directionality but better assessing differences in ranks across groups. We adopted these approaches and here refrain from interpreting whether a group has a lower/higher clustering or network density. Instead, we focus on the interesting finding that both mean clustering coefficient and network density – which capture how much a network tends to resemble a complete graph, cf. (Castro and Stella, 2019) – can result in measures differing between individuals with schizophrenia and controls, consistently across thresholds. The same pattern did not hold when comparing individuals with the bipolar disorder from controls. These differences might indicate alterations in the activation of regions of interest that we discussed in the sections above.

Our second key finding from the network analysis is that focusing on the local clustering coefficient of specific brain regions can highlight differences not only between individuals with schizophrenia and controls but also between the former and individuals with bipolar disorder. These regions have been investigated also in past studies (see specific

brain regions discussion). The local clustering coefficient can be considered as a local measure because it involves only one node and its neighbors (Castro and Stella, 2019). However, in networks as small as the ones investigated here and given that the node tIV9 belongs to the centre of a star graph involving all other nodes as neighbors (see Fig. 6), the local clustering coefficient of iTV9 might be considered as the outcome of the activation of several other brain regions being altered in individuals with schizophrenia. Interestingly, our quantitative patterns indicate that the neural activity captured via local clustering for regions iTV9 and iTV14 might be important for detecting altered patterns in schizophrenic individuals, with relevant repercussions for therapeutic and biomarking interventions.

To sum up, our findings provide compelling quantitative evidence that: (i) independently on the considered pathology, there are network-level patterns, encoded from brain activation levels, that are common to all the three considered groups, both at group-level (see Fig. S2) and persist also within individual-level networks (see Table 2–3), these patterns might represent basic biological activation circuits uninfluenced by pathologies; (ii) considering different thresholds corresponded to richer network structures, which highlighted differences in network-level features, like clustering or density, across pathologies; (iii) there are also node-level differences, where specific brain regions/nodes display considerable differences in their local clustering and degree of connectivity with other regions/nodes across the different groups. These findings underscore that: (i) complex networks might be capturing different circuits of brain activation signals as influenced by the presence/absence of key neural patterns characterizing schizophrenia and bipolar disorder, (ii) it is important to tune and test multiple threshold selections when performing network analyses of neuroimaging data. While a higher threshold may overlook subtle differences, more sensitive thresholds can unveil critical distinctions and commonalities in brain network architecture. This nuanced understanding could be pivotal in illuminating the underlying neuropathology of psychiatric conditions and informing targeted therapeutic strategies.

5. Study limitations

The study acknowledges several limitations. There was only partial confirmation of the affective core at a brain level, particularly in BD. The study dataset lacked psychosis-related measures, necessitating further research to characterize the psychosis continuum from a normal to a pathological population. Additionally, the analyses did not reveal significant subcortical differences between groups, possibly due to gray matter alterations linked to pharmacological treatments. In terms of network structure, selecting one threshold is a limitation, partially addressed here by considering and comparing multiple thresholds at once. Future approaches might build networks from data with information-theoretic approaches (Marinazzo et al., 2024). Moreover, although patients with schizophrenia and bipolar disorder were taking psychotropic medications (see Salvador et al., 2017 for details), we were not able to control for the potential effects of these variables on the significant networks identified. While the influence of psychotropic drugs is generally considered more evident at the functional level (Zhong et al., 2024), it is still possible that such medications may also have impacted brain structure (Ho et al., 2011). Future studies are needed to better control for this aspect. Another limitation of the present work lies in the use of brain scans acquired with a 1.5 Tesla MRI scanner. Although available evidence indicates that 1.5 Tesla scanners are widely regarded as sufficient for high-quality structural brain imaging in both clinical and research settings—and offer comparable performance to 3.0 Tesla scanners (Wood et al., 2012)—future research may wish to replicate and extend the present findings using higher-field scans. A further limitation pertains to the clinical heterogeneity within our patient groups, particularly the bipolar disorder (BD) cohort, which included individuals scanned during euthymic, manic, or depressive states. While our study focuses on structural MRI data (gray and white matter volumes), which are generally considered to reflect more stable, trait-like brain characteristics less susceptible to acute state fluctuations than functional measures, we cannot entirely rule out potential subtle influences of the current mood state on brain structure. Although we aimed to identify enduring neuroanatomical patterns, future longitudinal research would be beneficial to explicitly disentangle trait structural abnormalities from any state-dependent modulations within BD, and to assess how these relate to the continuum model with schizophrenia.

6. Conclusion

The present study aimed to elucidate the neural commonalities and differences between schizophrenia (SZ) and bipolar disorder (BD) to shed further light on the expanded continuum hypothesis proposed by Sorella et al. (2019). Using a data fusion unsupervised machine learning approach and network analyses to neuroimaging data, we identified a common neural substrate in a fronto-temporal network. These findings provide evidence of common neural alterations underlying SCZ and BD when compared to controls.

However, distinct structural abnormalities were also observed, with SCZ patients showing reduced GM-WM inside the cerebellum and medial frontal regions, absent in BD. These differences suggest divergent neural mechanisms across the two disorders. Network analysis confirmed a large deviation in SZ compared to CTRL but not in BD, further speaking for a large compromission of SZ compared to BD.

Future research should further explore these similarities and differences, considering also affective, and cognitive dimensions and how they share or differ in SZ and BD. Such investigations could refine diagnostic criteria and pave the way for more personalized treatment approaches tailored to the unique features of SCZ and BD.

CRediT authorship contribution statement

Alessandro Grecucci: Writing – review & editing, Writing – original draft, Visualization, Methodology, Formal analysis, Conceptualization. **Alessandro Scarano:** Writing – review & editing, Writing – original draft, Visualization, Methodology, Formal analysis, Conceptualization. **Francesco Bruno:** Writing – review & editing, Writing – original draft. **Gerardo Salvato:** Writing – review & editing, Writing – original draft. **Xiaoping Yi:** Writing – review & editing, Writing – original draft. **Massimo Stella:** Writing – review & editing, Writing – original draft, Formal analysis.

Funding

This research did not receive any fund, grant or other support from funding agencies in the public, commercial, or not-for-profit sectors.

Declaration of competing interest

The authors declare that they have no known competing financial interests or personal relationships that could have appeared to influence the work reported in this paper.

Data availability

Data are available at https://zenodo.org/records/460878

References

Adali, T., Levin-Schwartz, Y., Calhoun, V.D., 2015. Multi-modal data fusion using source separation: two effective models based on ICA and IVA and their properties. Proceedings of the IEEE. Institute of Electrical and Electronics Engineers 103 (9), 1478–1493. https://doi.org/10.1109/JPROC.2015.2461624.

Alba-Ferrara, L.M., de Erausquin, G.A., 2013 Mar 11. What does anisotropy measure? Insights from increased and decreased anisotropy in selective fiber tracts in

schizophrenia. Front. Integr. Neurosci. 7, 9. https://doi.org/10.3389/fnint.2013.00009.
Aleman, A., Kahn, R.S., 2005. Strange feelings: do amygdala abnormalities dysregulate the emotional brain in schizophrenia? Prog. Neurobiol. 77 (5), 283–298. https://doi.org/10.1016/j.pneurobio.2005.11.005.
American Psychiatric Association, D. S. M. T. F., & American Psychiatric Association, D. S, 2013. Diagnostic and Statistical Manual of Mental Disorders: DSM-5 (Vol. 5, No. 5). American Psychiatric Association, Washington, DC.
Arnone, D., Cavanagh, J., Gerber, D., Lawrie, S.M., Ebmeier, K.P., McIntosh, A.M., 2009 Sep. Magnetic resonance imaging studies in bipolar disorder and schizophrenia: meta-analysis. Br. J. Psychiatry 195 (3), 194–201. https://doi.org/10.1192/bjp.bp.108.059717.
Ashburner, J., 2009 Oct. Computational anatomy with the SPM software. Magn. Reson. Imaging 27 (8), 1163–1174. https://doi.org/10.1016/j.mri.2009.01.006 (Epub 2009 Feb 27).
Assaf, Y., Pasternak, O., 2008. Diffusion tensor imaging (DTI)-based white matter mapping in brain research: a review. J. Mol. Neurosci. 34 (1), 51–61. https://doi.org/10.1007/s12031-007-0029-0.
Baggio, T., Grecucci, A., Meconi, F., Messina, I., 2023 Jan 5. Anxious brains: a combined data fusion machine learning approach to predict trait anxiety from morphometric features. Sensors (Basel) 23 (2), 610. https://doi.org/10.3390/s23020610 (PMID: 36679404).
Barch, D.M., Ceaser, A., 2012 Jan. Cognition in schizophrenia: core psychological and neural mechanisms. Trends Cogn. Sci. 16 (1), 27–34. https://doi.org/10.1016/j.tics.2011.11.015 (Epub 2011 Dec 12. PMID: 22169777; PMCID: PMC3860986).
Benedetti, F., Absinta, M., Rocca, M.A., Radaelli, D., Poletti, S., Bernasconi, A., Dallaspezia, S., Pagani, E., Falini, A., Copetti, M., Colombo, C., Comi, G., Smeraldi, E., Filippi, M., 2011. Tract-specific white matter structural disruption in patients with bipolar disorder. Bipolar Disord. 13 (4), 414–424. https://doi.org/10.1111/j.1399-5618.2011.00938.x.
Bielawski, M., Bondurant, H., 2015. Psychosis following a stroke to the cerebellum and midbrain: a case report. Cerebellum & ataxias 2, 17. https://doi.org/10.1186/s40673-015-0037-8.
Biswal, B.B., Mennes, M., Zuo, X.N., Gohel, S., Kelly, C., Smith, S.M., Beckmann, C.F., Adelstein, J.S., Buckner, R.L., Colcombe, S., Dogonowski, A.M., Ernst, M., Fair, D., Hampson, M., Hoptman, M.J., Hyde, J.S., Kiviniemi, V.J., Kötter, R., Li, S.J., Lin, C. P., Lowe, M.J., Mackay, C., Madden, D.J., Madsen, K.H., Margulies, D.S., Mayberg, H.S., McMahon, K., Monk, C.S., Mostofsky, S.H., Nagel, B.J., Pekar, J.J., Peltier, S.J., Petersen, S.E., Riedl, V., Rombouts, S.A., Rypma, B., Schlaggar, B.L., Schmidt, S., Seidler, R.D., Siegle, G.J., Sorg, C., Teng, G.J., Veijola, J., Villringer, A., Walter, M., Wang, L., Weng, X.C., Whitfield-Gabrieli, S., Williamson, P., Windischberger, C., Zang, Y.F., Zhang, H.Y., Castellanos, F.X., Milham, M.P., 2010 Mar 9. Toward discovery science of human brain function. Proc. Natl. Acad. Sci. USA 107 (10), 4734–4739. https://doi.org/10.1073/pnas.0911855107.
Bora, E., Pantelis, C., 2015. Meta-analysis of cognitive impairment in first-episode bipolar disorder: comparison with first-episode schizophrenia and healthy controls. Schizophrenia Bull. 41 (5), 1095–1104. https://doi.org/10.1093/schbul/sbu198.
Bora, E., Yucel, M., Pantelis, C., 2009. Cognitive endophenotypes of bipolar disorder: a meta-analysis of neuropsychological deficits in euthymic patients and their first-degree relatives. J. Affect. Disord. 113 (1–2), 1–20. https://doi.org/10.1016/j.jad.2008.06.009.
Bortolato, B., Miskowiak, K., Vieta, E., Köhler, C., Carvalho, A.F., 2015. Cognitive dysfunction in bipolar disorder and schizophrenia: a systematic review of meta-analyses. Neuropsychiatr. Dis. Treat. 11, 3111. https://doi.org/10.2147/ndt.s76700.
Bowie, C.R., Bell, M.D., Fiszdon, J.M., Johannesen, J.K., Lindenmayer, J.P., McGurk, S. R., Medalia, A.A., Penadés, R., Saperstein, A.M., Twamley, E.W., Ueland, T., Wykes, T., 2020 Jan. Cognitive remediation for schizophrenia: an expert working group white paper on core techniques. Schizophr. Res. 215, 49–53. https://doi.org/10.1016/j.schres.2019.10.047.
Breiman, L., 2001. Using iterated bagging to Debias regressions. Mach. Learn. 45, 261–277. https://doi.org/10.1023/A:1017934522171.
Butler, P.D., Silverstein, S.M., Dakin, S.C., 2008. Visual perception and its impairment in schizophrenia. Biol. Psychiatry 64 (1), 40–47. https://doi.org/10.1016/j.biopsych.2008.03.023.
Calhoun, V.D., Adali, T., Kiehl, K.A., Astur, R., Pekar, J.J., Pearlson, G.D., 2006. A method for multitask fMRI data fusion applied to schizophrenia. Hum. Brain Mapp. 27 (7), 598–610. https://doi.org/10.1002/hbm.20204.
Castro, N., Stella, M., 2019. The multiplex structure of the mental lexicon influences picture naming in people with aphasia. J. Complex Netw. 7 (6), 913–931.
Cheng, Y., Cai, H., Liu, S., Yang, Y., Pan, S., Zhang, Y., Mo, F., Yu, Y., Zhu, J., 2025. Brain network localization of gray matter atrophy and neurocognitive and social cognitive dysfunction in schizophrenia. Biol. Psychiatry 97 (2), 148–156. https://doi.org/10.1016/j.biopsych.2024.07.021.
Conio, B., Martino, M., Magioncalda, P., Escelsior, A., Inglese, M., Amore, M., Northoff, G., 2020. Opposite effects of dopamine and serotonin on resting-state networks: review and implications for psychiatric disorders. Mol. Psychiatry 25 (1), 82–93. https://doi.org/10.1038/s41380-019-0406-4.
Craddock, N., Owen, M.J., 2010. The genetics of bipolar disorder. Nat. Rev. Genet. 11 (5), 365–374.
Diederen, K.M., Neggers, S.F., Daalman, K., Blom, J.D., Goekoop, R., Kahn, R.S., Sommer, I.E., 2010. Deactivation of the parahippocampal gyrus preceding auditory hallucinations in schizophrenia. Am. J. Psychiatry 167 (4), 427–435. https://doi.org/10.1176/appi.ajp.2009.09040456.
Dong, D., Wang, Y., Chang, X., Luo, C., Yao, D., 2018. Dysfunction of large-scale brain networks in schizophrenia: a meta-analysis of resting-state functional connectivity. Schizophr. Bull. 44 (1), 168–181. https://doi.org/10.1093/schbul/sbx034.
Doniger, G.M., Foxe, J.J., Murray, M.M., Higgins, B.A., Javitt, D.C., 2002. Impaired visual object recognition and dorsal/ventral stream interaction in schizophrenia. Arch. Gen. Psychiatry 59 (11), 1011. https://doi.org/10.1001/archpsyc.59.11.1011.
Ellison-Wright, I., Bullmore, E., 2010 Mar. Anatomy of bipolar disorder and schizophrenia: a meta-analysis. Schizophr. Res. 117 (1), 1–12. https://doi.org/10.1016/j.schres.2009.12.022 (Epub 2010 Jan 13).
van Erp, T.G., Hibar, D.P., Rasmussen, J.M., Glahn, D.C., Pearlson, G.D., Andreassen, O. A., Agartz, I., Westlye, L.T., Haukvik, U.K., Dale, A.M., Melle, I., Hartberg, C.B., Gruber, O., Kraemer, B., Zilles, D., Donohoe, G., Kelly, S., McDonald, C., Morris, D. W., Cannon, D.M., 2016. Subcortical brain volume abnormalities in 2028 individuals with schizophrenia and 2540 healthy controls via the ENIGMA consortium. Mol. Psychiatry 21 (4), 547–553. https://doi.org/10.1038/mp.2015.63.
Fernandes, T.M.P., Andrade, S.M., de Andrade, M.J.O., Nogueira, R.M.T.B.L., Santos, N. A., 2017. Colour discrimination thresholds in type 1 bipolar disorder: a pilot study. Sci. Rep. 7 (1). https://doi.org/10.1038/s41598-017-16752-0.
Ffytche, D.H., Wible, C.G., 2014. From tones in tinnitus to sensed social interaction in schizophrenia: how understanding cortical organization can inform the study of hallucinations and psychosis. Schizophrenia Bull. 40. https://doi.org/10.1093/schbul/sbu041.
Fortuna, A., Ferrante, L., Lunardi, P., 2001. Brain tumors. In: Essential Illustrated Neurosurgery. Springer, pp. 9–58. https://doi.org/10.1007/978-88-470-2908-8_2.
Fox, M.D., Snyder, A.Z., Vincent, J.L., Corbetta, M., Van Essen, D.C., Raichle, M.E., 2005. The human brain is intrinsically organized into dynamic, anticorrelated functional networks. Proc. Natl. Acad. Sci. USA 102 (27), 9673–9678. https://doi.org/10.1073/pnas.0504136102.
Garrity, A.G., Pearlson, G.D., McKiernan, K., Lloyd, D., Kiehl, K.A., Calhoun, V.D., 2007. Aberrant "default mode" functional connectivity in schizophrenia. Am. J. Psychiatry 164 (3), 450–457. https://doi.org/10.1176/ajp.2007.164.3.450.
Goldsmith, D.R., Rapaport, M.H., Miller, B.J., 2016 Dec. A meta-analysis of blood cytokine network alterations in psychiatric patients: comparisons between schizophrenia, bipolar disorder and depression. Mol. Psychiatry 21 (12), 1696–1709. https://doi.org/10.1038/mp.2016.3 (Epub 2016 Feb 23. PMID: 26903267; PMCID: PMC6056174).
Grecucci, A., Rubicondo, D., Siugzdaite, R., Surian, L., Job, R., 2016. Uncovering social deficits in autistic individuals: a source-based morphometry study. Front. Neurosci. 31, 10.
Grecucci, A., Siugzdaite, R., Job, R., 2017. Editorial: advanced neuroimaging methods for studying autism disorder. Front. Hum. Neurosci. (Special issue.388).
Grecucci, A., Sorella, S., Consolini, J., 2022. Decoding individual differences in expressing and suppressing anger from structural brain networks: a supervised machine learning approach. Behav. Brain Res. 439, 114245.
Grecucci, A., Orsini, C., Lapomarda, G., Sorella, S., Messina, I., 2023. Perceiving visual negative stimuli in schizophrenia and bipolar disorder: Meta-analytic evidence of a common altered thalamic-parahippocampal-basal ganglia circuit. Neuroimage: Reports 3 (2). https://doi.org/10.1016/j.ynirp.2023.100173.
Groves, A.R., Beckmann, C.F., Smith, S.M., Woolrich, M.W., 2011. Linked independent component analysis for multimodal data fusion. NeuroImage 54 (3), 2198–2217. https://doi.org/10.1016/j.neuroimage.2010.09.073.
Gupta, C.N., Calhoun, V.D., Rachakonda, S., Chen, J., Patel, V., Liu, J., Segall, J., Franke, B., Zwiers, M.P., Arias-Vasquez, A., Buitelaar, J., Fisher, S.E., Fernandez, G., van Erp, T.G., Potkin, S., Ford, J., Mathalon, D., McEwen, S., Lee, H.J., Mueller, B.A., Turner, J.A., 2015. Patterns of gray matter abnormalities in schizophrenia based on an international mega-analysis. Schizophr. Bull. 41 (5), 1133–1142. https://doi.org/10.1093/schbul/sbu177.
Haber, S.N., 2014. The place of dopamine in the cortico-basal ganglia circuit. Neuroscience 282, 248–257. https://doi.org/10.1016/j.neuroscience.2014.10.008.
Haber, S.N., Knutson, B., 2010. The reward circuit: linking primate anatomy and human imaging. Neuropsychopharmacology 35 (1), 4–26. https://doi.org/10.1038/npp.2009.129.
Hajek, T., Alda, M., Hajek, E., Ivanoff, J., 2013. Functional neuroanatomy of response inhibition in bipolar disorders–combined voxel based and cognitive performance meta-analysis. J. Psychiatr. Res. 47 (12), 1955–1966. https://doi.org/10.1016/j.jpsychires.2013.08.015.
Hastie, T., Tibshirani, R., Friedman, J., 2001. The Elements of Statistical Learning. Springer New York, NY. https://doi.org/10.1007/978-0-387-84858-7.
Hebart, M.N., Baker, C.I., 2018 Oct 15. Deconstructing multivariate decoding for the study of brain function. Neuroimage 180 (Pt A), 4–18. https://doi.org/10.1016/j.neuroimage.2017.08.005 (Epub 2017 Aug 4).
Heng, S., Song, A.W., Sim, K., 2010. White matter abnormalities in bipolar disorder: insights from diffusion tensor imaging studies. J. Neural Transm. 117, 639–654. https://doi.org/10.1007/s00702-010-0368-9.
Herbener, E.S., 2008. Emotional memory in schizophrenia. Schizophr. Bull. 34 (5), 875–887. https://doi.org/10.1093/schbul/sbn081.
van den Heuvel, M.P., Sporns, O., 2013. Network hubs in the human brain. Trends Cogn. Sci. 17 (12), 683–696. https://doi.org/10.1016/j.tics.2013.09.012.
Himberg, J., Hyvärinen, A., Esposito, F., 2004 Jul. Validating the independent components of neuroimaging time series via clustering and visualization. Neuroimage 22 (3), 1214–1222. https://doi.org/10.1016/j.neuroimage.2004.03.027.
Hirjak, D., Wolf, R.C., Wilder-Smith, E.P., Kubera, K.M., Thomann, P.A., 2015. Motor abnormalities and basal ganglia in schizophrenia: evidence from structural magnetic resonance imaging. Brain Topogr. 28 (1), 135–152. https://doi.org/10.1007/s10548-014-0377-3.
Ho, T.K., 1998. The random subspace method for constructing decision forests. IEEE Trans. Pattern Anal. Mach. Intell. 20, 832–844. https://doi.org/10.1109/34.709601.

Ho, B.C., Andreasen, N.C., Ziebell, S., Pierson, R., Magnotta, V., 2011. Long-term antipsychotic treatment and brain volumes: a longitudinal study of first-episode schizophrenia. Arch. Gen. Psychiatry 68 (2), 128–137. https://doi.org/10.1001/archgenpsychiatry.2010.199.

Honey, C.J., Sporns, O., Cammoun, L., Gigandet, X., Thiran, J.P., Meuli, R., Hagmann, P., 2009. Predicting human resting-state functional connectivity from structural connectivity. Proc. Natl. Acad. Sci. U. S. A. 106 (6), 2035–2040. https://doi.org/10.1073/pnas.0811168106.

Horga, G., Bernacer, J., Dusi, N., Entis, J., Chu, K., Hazlett, E.A., Haznedar, M.M., Kemether, E., Byne, W., Buchsbaum, M.S., 2011. Correlations between ventricular enlargement and gray and white matter volumes of cortex, thalamus, striatum, and internal capsule in schizophrenia. Eur. Arch. Psychiatry Clin. Neurosci. 261 (7), 467–476. https://doi.org/10.1007/s00406-011-0202-x.

Howes, O.D., Kapur, S., 2009. The dopamine hypothesis of schizophrenia: version III–the final common pathway. Schizophr. Bull. 35 (3), 549–562. https://doi.org/10.1093/schbul/sbp006.

Hwang, J., Lyoo, I.K., Dager, S.R., Friedman, S.D., Oh, J.S., Lee, J.Y., Kim, S.J., Dunner, D.L., Renshaw, P.F., 2006. Basal ganglia shape alterations in bipolar disorder. Am. J. Psychiatry 163 (2), 276–285. https://doi.org/10.1176/appi.ajp.163.2.276.

Jenkinson, M., Beckmann, C.F., Behrens, T.E.J., Woolrich, M.W., Smith, S.M., 2012. FSL, NeuroImage 62 (2), 782–790. ISSN 1053-8119. https://doi.org/10.1016/j.neuroimage.2011.09.015. https://www.sciencedirect.com/science/article/pii/S1053811911010603.

Kanaan, R., Barker, G., Brammer, M., Giampietro, V., Shergill, S., Woolley, J., Picchioni, M., Toulopoulou, T., McGuire, P., 2009. White matter microstructure in schizophrenia: effects of disorder, duration and medication. Br. J. Psychiatry J. Ment. Sci. 194 (3), 236–242. https://doi.org/10.1192/bjp.bp.108.054320.

Kapur, S., 2003. Psychosis as a state of aberrant salience: a framework linking biology, phenomenology, and pharmacology in schizophrenia. Am. J. Psychiatry 160 (1), 13–23. https://doi.org/10.1176/appi.ajp.160.1.13.

Kasparek, T., Marecek, R., Schwarz, D., Prikryl, R., Vanícek, J., Mikl, M., Cesková, E., 2010. Source-based morphometry of gray matter volume in men with first-episode schizophrenia. Hum. Brain Mapp. 31, 300–310. https://doi.org/10.1002/hbm.20865.

Khantzian, E.J., 1997. The self-medication hypothesis of substance use disorders: a reconsideration and recent applications. Harv. Rev. Psychiatry 4 (5), 231–244.

Kim, S.E., Jung, S., Sung, G., et al., 2021. Impaired cerebro-cerebellar white matter connectivity and its associations with cognitive function in patients with schizophrenia. NPJ Schizophr. 7 (38). https://doi.org/10.1038/s41537-021-00169-w.

Koch, K., Wagner, G., Dahnke, R., Schachtzabel, C., Schultz, C., Roebel, M., Güllmar, D., Reichenbach, J.R., Sauer, H., Schlösser, R.G., 2010. Disrupted white matter integrity of corticopontine-cerebellar circuitry in schizophrenia. Eur. Arch. Psychiatry Clin. Neurosci. 260 (5), 419–426. https://doi.org/10.1007/s00406-009-0087-0.

Kohler, C.G., Martin, E.A., 2006. Emotional processing in schizophrenia. Cognit. Neuropsychiatry 11 (3), 250–271. https://doi.org/10.1080/13546800500188575.

Krabbendam, L., Arts, B., van Os, J., Aleman, A., 2005. Cognitive functioning in patients with schizophrenia and bipolar disorder: a quantitative review. Schizophr. Res. 80 (2–3), 137–149. https://doi.org/10.1016/j.schres.2005.08.004.

Kumral, E., Ozturk, O., 2004. Delusional state following acute stroke. Neurology 62 (1), 110–113. https://doi.org/10.1212/wnl.62.1.110.

Laidi, C., d'Albis, M., Wessa, M., Linke, J., Phillips, M.L., Delavest, M., Houenou, J., 2015. Cerebellar volume in schizophrenia and bipolar I disorder with and without psychotic features. Acta Psychiatr. Scand. 131 (3), 223–233. https://doi.org/10.1111/acps.12363.

Laloyaux, J., De Keyser, F., Pinchard, A., Della Libera, C., Larøi, F., 2019. Testing a model of auditory hallucinations: the role of negative emotions and cognitive resources. Cogn. Neuropsychiatry 24 (4), 256–274. https://doi.org/10.1080/13546805.2019.1629895.

Lapomarda, G., Grecucci, A., Messina, I., Pappaianni, E., Dadomo, H., 2021a. Common and different gray and white matter alterations in bipolar and borderline personality disorder: a source-based morphometry study. Brain Res. 1762, 147401. https://doi.org/10.1016/j.brainres.2021.147401.

Lapomarda, G., Pappaianni, E., Siugzdaite, R., Sanfey, A.G., Rumiati, R.I., Grecucci, A., 2021b. Out of control: an altered parieto-occipital-cerebellar network for impulsivity in bipolar disorder. Behav. Brain Res. 406, 113228. https://doi.org/10.1016/j.bbr.2021.113228.

Lee, J.H., Lee, T.W., Jolesz, F.A., Yoo, S.S., 2008. Independent vector analysis (IVA): multivariate approach for fMRI group study. NeuroImage 40 (1), 86–109. https://doi.org/10.1016/j.neuroimage.2007.11.019.

Leech, R., Sharp, D.J., 2013. The role of the posterior cingulate cortex in cognition and disease. Brain 137 (1), 12–32. https://doi.org/10.1093/brain/awt162.

Lewandowski, K.E., Cohen, B.M., Ongur, D., 2011 Feb. Evolution of neuropsychological dysfunction during the course of schizophrenia and bipolar disorder. Psychol. Med. 41 (2), 225–241. https://doi.org/10.1017/S0033291710001042 (Epub 2010 May 19).

Li, P., Zhao, S.W., Wu, X.S., Zhang, Y.J., Song, L., Wu, L., Liu, X.F., Fu, Y.F., Wu, D., Wu, W.J., Zhang, Y.H., Yin, H., Cui, L.B., Guo, F., 2021. The association between lentiform nucleus function and cognitive impairments in schizophrenia. Front. Hum. Neurosci. 15, 777043. https://doi.org/10.3389/fnhum.2021.777043.

Lochhead, R.A., Parsey, R.V., Oquendo, M.A., Mann, J.J., 2004. Regional brain gray matter volume differences in patients with bipolar disorder as assessed by optimized voxel-based morphometry. Biol. Psychiatry 55, 1154–1162. https://doi.org/10.1016/j.biopsych.2004.02.026.

Logothetis, N.K., Pauls, J., Poggio, T., 1995. Shape representation in the inferior temporal cortex of monkeys. Curr. Biol. 5 (5), 552–563. https://doi.org/10.1016/s0960-9822(95)00108-4.

Maggioni, E., Crespo-Facorro, B., Nenadic, I., Benedetti, F., Gaser, C., Sauer, H., Roiz-Santiañez, R., Poletti, S., Marinelli, V., Bellani, M., Perlini, C., Ruggeri, M., Altamura, A.C., Diwadkar, V.A., Brambilla, P., ENPACT Group, 2017 Nov 14. Common and distinct structural features of schizophrenia and bipolar disorder: the European network on psychosis, affective disorders and cognitive trajectory (ENPACT) study. PLoS One 12 (11), e0188000. https://doi.org/10.1371/journal.pone.0188000.

Magioncalda, P., Martino, M., Conio, B., Lee, H.C., Ku, H.L., Chen, C.J., Inglese, M., Amore, M., Lane, T.J., Northoff, G., 2020. Intrinsic brain activity of subcortical-cortical sensorimotor system and psychomotor alterations in schizophrenia and bipolar disorder: a preliminary study. Schizophr. Res. 218, 157–165. https://doi.org/10.1016/j.schres.2020.01.009.

Mahon, K., Burdick, K.E., Szeszko, P.R., 2010. A role for white matter abnormalities in the pathophysiology of bipolar disorder. Neurosci. Biobehav. Rev. 34 (4), 533–554. https://doi.org/10.1016/j.neubiorev.2009.10.012.

Mamah, D., Wang, L., Barch, D., de Erausquin, G.A., Gado, M., Csernansky, J.G., 2007. Structural analysis of the basal ganglia in schizophrenia. Schizophr. Res. 89 (1–3), 59–71. https://doi.org/10.1016/j.schres.2006.08.031.

Marinazzo, D., Van Roozendaal, J., Rosas, F.E., Stella, M., Comolatti, R., Colenbier, N., Rosseel, Y., 2024. An information-theoretic approach to build hypergraphs in psychometrics. Behav. Res. Methods 56 (7), 8057–8079. https://doi.org/10.3758/s13428-024-02471-8.

McDonald, B., Highley, J.R., Walker, M.A., Herron, B.M., Cooper, S.J., Esiri, M.M., Crow, T.J., 2000. Anomalous asymmetry of fusiform and Parahippocampal gyrus gray matter in schizophrenia: a postmortem study. Am. J. Psychiatry 157 (1), 40–47. https://doi.org/10.1176/ajp.157.1.40.

McIntosh, A.M., Job, D.E., Moorhead, T.W., Harrison, L.K., Forrester, K., Lawrie, S.M., Johnstone, E.C., 2004 Oct 15. Voxel-based morphometry of patients with schizophrenia or bipolar disorder and their unaffected relatives. Biol. Psychiatry 56 (8), 544–552. https://doi.org/10.1016/j.biopsych.2004.07.020.

McIntosh, A.M., Muñoz Maniega, S., Lymer, G.K., McKirdy, J., Hall, J., Sussmann, J.E., Bastin, M.E., Clayden, J.D., Johnstone, E.C., Lawrie, S.M., 2008. White matter tractography in bipolar disorder and schizophrenia. Biol. Psychiatry 64 (12), 1088–1092. https://doi.org/10.1016/j.biopsych.2008.07.026.

McLaughlin, R.L., Schijven, D., van Rheenen, W., van Eijk, K.R., O'Brien, M., Kahn, R.S., Ophoff, R.A., Goris, A., Bradley, D.G., Al-Chalabi, A., van den Berg, L.H., Luykx, J.J., Hardiman, O., Veldink, J.H., Project MinE GWAS Consortium, 2017 Mar 21. Schizophrenia working Group of the Psychiatric Genomics Consortium. Genetic correlation between amyotrophic lateral sclerosis and schizophrenia. Nat. Commun. 8, 14774. https://doi.org/10.1038/ncomms14774.

Meda, S.A., Gill, A., Stevens, M.C., Lorenzoni, R.P., Glahn, D.C., Calhoun, V.D., Sweeney, J.A., Tamminga, C.A., Keshavan, M.S., Thaker, G., Pearlson, G.D., 2012. Differences in resting-state functional magnetic resonance imaging functional network connectivity between schizophrenia and psychotic bipolar probands and their unaffected first-degree relatives. Biol. Psychiatry 71 (10), 881–889. https://doi.org/10.1016/j.biopsych.2012.01.025.

Meer, L.V., Vos, A.E., Stiekema, A.P., Pijnenborg, G.H., Tol, M.V., Nolen, W.A., Aleman, A., 2012. Insight in schizophrenia: involvement of self-reflection networks? Schizophr. Bull. 39 (6), 1288–1295. https://doi.org/10.1093/schbul/sbs122.

Miller, S., Dell'Osso, B., Ketter, T.A., 2014 Dec. The prevalence and burden of bipolar depression. J. Affect. Disord. 169 (Suppl 1), S3–11. https://doi.org/10.1016/S0165-0327(14)70003-5 (PMID: 25533912).

Minzenberg, M.J., Laird, A.R., Thelen, S., Carter, C.S., Glahn, D.C., 2009. Meta-analysis of 41 functional neuroimaging studies of executive function in schizophrenia. Arch. Gen. Psychiatry 66 (8), 811. https://doi.org/10.1001/archgenpsychiatry.2009.91.

Mo, F., Zhao, H., Li, Y., Cai, H., Song, Y., Wang, R., Yu, Y., Zhu, J., 2024. Network localization of state and trait of auditory verbal hallucinations in schizophrenia. Schizophr. Bull. 50 (6), 1326–1336. https://doi.org/10.1093/schbul/sbae020.

Modinos, G., Costafreda, S.G., van Tol, M.J., McGuire, P.K., Aleman, A., Allen, P., 2013. Neuroanatomy of auditory verbal hallucinations in schizophrenia: a quantitative meta-analysis of voxel-based morphometry studies. Cortex 49 (4), 1046–1055. https://doi.org/10.1016/j.cortex.2012.01.009.

Moghaddam, B., Javitt, D., 2012. From revolution to evolution: the glutamate hypothesis of schizophrenia and its implication for treatment. Neuropsychopharmacology 37 (1), 4–15.

Molina, J., Sikora, M., Garud, N., Flowers, J.M., Rubinstein, S., Reynolds, A., Huang, P., Jackson, S., Schaal, B.A., Bustamante, C.D., Boyko, A.R., Purugganan, M.D., 2011 May 17. Molecular evidence for a single evolutionary origin of domesticated rice. Proc. Natl. Acad. Sci. USA 108 (20), 8351–8356. https://doi.org/10.1073/pnas.1104686108 (Epub 2011 May 2).

Moller, H.J., 2003. Bipolar disorder and schizophrenia: distinct illnesses or a continuum? J. Clin. Psychiatry 64, 23–27.

Nenadic, I., Dietzek, M., Schönfeld, N., Lorenz, C., Gussew, A., Reichenbach, J.R., Sauer, H., Gaser, C., Smesny, S., 2015 Feb. Brain structure in people at ultra-high risk of psychosis, patients with first-episode schizophrenia, and healthy controls: a VBM study. Schizophr. Res. 161 (2–3), 169–176. https://doi.org/10.1016/j.schres.2014.10.041 (Epub 2014 Dec 12).

Newman, M., 2018. Networks. Oxford University Press.

O'Bryan, R.A., Brenner, C.A., Hetrick, W.P., O'Donnell, B.F., 2014. Disturbances of visual motion perception in bipolar disorder. Bipolar Disord. 16 (4), 354–365. https://doi.org/10.1111/bdi.12173.

Pappaianni, E., Siugzdaite, R., Vettori, S., Venuti, P., Job, R., Grecucci, A., 2018. Three shades of grey: detecting brain abnormalities in children with autism by using source-, voxel- and surface-based morphometry. Eur. J. Neurosci. 47 (6), 690–700.
Rabins, P.V., Starkstein, S.E., Robinson, R.G., 1991. Risk factors for developing atypical (schizophreniform) psychosis following stroke. J. Neuropsychiatry Clin. Neurosci. 3 (1), 6–9. https://doi.org/10.1176/jnp.3.1.6.
Radwan, A.M., Sunaert, S., Schilling, K., Descoteaux, M., Landman, B.A., Vandenbulcke, M., Theys, T., Dupont, P., Emsell, L., 2022 Jul 1. An atlas of white matter anatomy, its variability, and reproducibility based on constrained spherical deconvolution of diffusion MRI. Neuroimage 254, 119029. https://doi.org/10.1016/j.neuroimage.2022.119029 (Epub 2022 Feb 26).
Regier, D.A., Farmer, M.E., Rae, D.S., Locke, B.Z., Keith, S.J., Judd, L.L., Goodwin, F.K., 1990. Comorbidity of mental disorders with alcohol and other drug abuse: results from the Epidemiologic Catchment Area (ECA) study. JAMA 264 (19), 2511–2518.
Repovš, G., Barch, D.M., 2012. Working memory related brain network connectivity in individuals with schizophrenia and their siblings. Front. Hum. Neurosci. 6, 137. https://doi.org/10.3389/fnhum.2012.00137.
Rheenen, T.E., Bryce, S., Tan, E.J., Neill, E., Gurvich, C., Louise, S., Rossell, S.L., 2016. Does cognitive performance map to categorical diagnoses of schizophrenia, schizoaffective disorder and bipolar disorder? A discriminant functions analysis. J. Affect. Disord. 192, 109–115. https://doi.org/10.1016/j.jad.2015.12.022.
Rimol, L.M., Hartberg, C., Nesvåg, R., Fennema-Notestine, C., Hagler, D., Pung, C.J., Agartz, I., 2010. Cortical thickness and subcortical volumes in schizophrenia and bipolar disorder. Schizophr. Res. 117 (2–3), 459. https://doi.org/10.1016/j.schres.2010.02.857.
Rimol, L.M., Nesvåg, R., Hagler Jr., D.J., Bergmann, O., Fennema-Notestine, C., Hartberg, C.B., Haukvik, U.K., Lange, E., Pung, C.J., Server, A., Melle, I., Andreassen, O.A., Agartz, I., Dale, A.M., 2012 Mar 15. Cortical volume, surface area, and thickness in schizophrenia and bipolar disorder. Biol. Psychiatry 71 (6), 552–560. https://doi.org/10.1016/j.biopsych.2011.11.026 (Epub 2012 Jan 26. Erratum in: Biol Psychiatry. 2012 Apr 1;71(7):660).
Roberts, D.L., Tatini, U., Zimmerman, R.S., Bortz, J.J., Sirven, J.I., 2001. Musical hallucinations associated with seizures originating from an intracranial aneurysm. Mayo Clin. Proc. 76 (4), 423–426. https://doi.org/10.4065/76.4.423.
Rubinov, M., Sporns, O., 2010. Complex network measures of brain connectivity: uses and interpretations. NeuroImage 52 (3), 1059–1069. https://doi.org/10.1016/j.neuroimage.2009.10.003.
Salvador, R., Radua, J., Canales-Rodríguez, E.J., Solanes, A., Sarró, S., Goikolea, J.M., Valiente, A., Monté, G.C., Natividad, M.D.C., Guerrero-Pedraza, A., Moro, N., Fernández-Corcuera, P., Amann, B.L., Maristany, T., Vieta, E., McKenna, P.J., Pomarol-Clotet, E., 2017. Evaluation of machine learning algorithms and structural features for optimal MRI-based diagnostic prediction in psychosis. PloS One 12 (4), e0175683. https://doi.org/10.1371/journal.pone.0175683.
Samartzis, L., Dima, D., Fusar-Poli, P., & Kyriakopoulos, M. (2014). White matter alterations in early stages of schizophrenia: a systematic review of diffusion tensor imaging studies. J. Neuroimaging, 24(2), 101–110. doi:https://doi.org/10.1111/j.1552-6569.2012.00779.xSanches, M., Keshavan, M. S., Brambilla, P., & Soares, J. C. (2008). Neurodevelopmental basis of bipolar disorder: a critical appraisal. Prog. Neuropsychopharmacol. Biol. Psychiatry, 32(7), 1617–1627.
Seeman, P., Kapur, S., 2000. Schizophrenia: More dopamine, more D2 receptors. Proc. Natl. Acad. Sci. U. S. A. 97 (14), 7673–7675. https://doi.org/10.1073/pnas.97.14.7673.
Selva, G., Salazar, J., Balanzá-Martínez, V., Martínez-Arán, A., Rubio, C., Daban, C., Tabarés-Seisdedos, R., 2007. Bipolar I patients with and without a history of psychotic symptoms: do they differ in their cognitive functioning? J. Psychiatr. Res. 41 (3–4), 265–272. https://doi.org/10.1016/j.jpsychires.2006.03.007.
Smith, S.M., 2002 Nov. Fast robust automated brain extraction. Hum. Brain Mapp. 17 (3), 143–155. https://doi.org/10.1002/hbm.10062 (PMID: 12391568; PMCID: PMC6871816).
Spalletta, G., Musicco, M., Padovani, A., Rozzini, L., Perri, R., Fadda, L., Canonico, V., Trequattrini, A., Pettenati, C., Caltagirone, C., Palmer, K., 2010 Nov. Neuropsychiatric symptoms and syndromes in a large cohort of newly diagnosed, untreated patients with Alzheimer disease. Am. J. Geriatr. Psychiatry 18 (11), 1026–1035. https://doi.org/10.1097/JGP.0b013e3181d6b68d.
Sorella, S., Lapomarda, G., Messina, I., Frederickson, J.J., Siugzdaite, R., Job, R., Grecucci, A., 2019. Testing the expanded continuum hypothesis of schizophrenia and bipolar disorder. Neural and psychological evidence for shared and distinct mechanisms. NeuroImage: Clinical 23, 101854.
Sporns, O., 2016. Networks of the Brain. MIT Press.
Stangeland, H., Orgeta, V., Bell, V., 2018. Poststroke psychosis: a systematic review. J. Neurol. Neurosurg. Psychiatry 89 (8), 879–885. https://doi.org/10.1136/jnnp-2017-317327.
Stefanopoulou, E., Manoharan, A., Landau, S., Geddes, J.R., Goodwin, G., Frangou, S., 2009. Cognitive functioning in patients with affective disorders and schizophrenia: a meta-analysis. Int. Rev. Psychiatr. 21 (4), 336–356. https://doi.org/10.1080/09540260902962149.
Strakowski, S.M., 2014. Bipolar disorder. Oxford University Press.
Strakowski, S., DelBello, M., Adler, C., 2005. The functional neuroanatomy of bipolar disorder: a review of neuroimaging findings. Mol. Psychiatry 10 (1), 105–116. https://doi.org/10.1038/sj.mp.4001585.
Sui, J., He, H., Yu, Q., Chen, J., Rogers, J., Pearlson, G.D., Mayer, A., Bustillo, J., Canive, J., Calhoun, V.D., 2013. Combination of resting state fMRI, DTI, and sMRI data to discriminate schizophrenia by N-way MCCA + jICA. Front. Hum. Neurosci. 7, 235. https://doi.org/10.3389/fnhum.2013.00235.
Sullivan, P.F., Magnusson, C., Reichenberg, A., Boman, M., Dalman, C., Davidson, M., Lichtenstein, P., 2012. Family history of schizophrenia and bipolar disorder as risk factors for autism. Arch. Gen. Psychiatry 69 (11), 1099–1103.
Sussmann, J.E., Lymer, G.K., McKirdy, J., Moorhead, T.W., Muñoz Maniega, S., Job, D., Hall, J., Bastin, M.E., Johnstone, E.C., Lawrie, S.M., McIntosh, A.M., 2009. White matter abnormalities in bipolar disorder and schizophrenia detected using diffusion tensor magnetic resonance imaging. Bipolar Disord. 11 (1), 11–18. https://doi.org/10.1111/j.1399-5618.2008.00646.x.
Tandon, R., Keshavan, M.S., Nasrallah, H.A., 2013. Schizophrenia, "just the facts" 5. Treatment and prevention. Schizophr. Res. 140 (1–3), 7–16.
Toda, M., Abi-Dargham, A., 2007. Dopamine hypothesis of schizophrenia: making sense of it all. Curr. Psychiatr. Rep. 9 (4), 329–336. https://doi.org/10.1007/s11920-007-0041-7.
Townsend, J., Altshuler, L.L., 2012. Emotion processing and regulation in bipolar disorder: a review. Bipolar Disord. 14 (4), 326–339. https://doi.org/10.1111/j.1399-5618.2012.01021.x.
Trémeau, F., 2006. A review of emotion deficits in schizophrenia. Dialogues Clin. Neurosci. 8 (1), 59–70. https://doi.org/10.31887/DCNS.2006.8.1/ftremeau.
Vieira, S., Pinaya, W.H.L., Mechelli, A., 2020. Chapter 1 - Introduction to machine learning. In: Mechelli, A. (Ed.). Machine Learning, Academic Press, Sandra Vieira, ISBN 9780128157398, pp. 1–20. https://doi.org/10.1016/B978-0-12-815739-8.00001-8.
Vytal, K., Hamann, S., 2010. Neuroimaging support for discrete neural correlates of basic emotions: a voxel-based meta-analysis. J. Cogn. Neurosci. 22 (12), 2864–2885. https://doi.org/10.1162/jocn.2009.21366.
Waters, F., Allen, P., Aleman, A., Fernyhough, C., Woodward, T.S., Badcock, J.C., Barkus, E., Johns, L., Varese, F., Menon, M., Vercammen, A., Larøi, F., 2012. Auditory hallucinations in schizophrenia and nonschizophrenia populations: a review and integrated model of cognitive mechanisms. Schizophr. Bull. 38 (4), 683–693. https://doi.org/10.1093/schbul/sbs045.
Wood, R., Bassett, K., Foerster, 5th, Spry, C., Tong, L., 2012. 1.5 tesla magnetic resonance imaging scanners compared with 3.0 tesla magnetic resonance imaging scanners: systematic review of clinical effectiveness. CADTH Technol Overv. 2 (2), e2201.
World Health Organization, 1993. The ICD–10 Classification of Mental and Behavioural Disorders–Diagnostic Criteria for Research. WHO, Geneva.
Xu, R., Zhang, X., Zhou, S., Guo, L., Mo, F., Ma, H., Zhu, J., Qian, Y., 2024. Brain structural damage networks at different stages of schizophrenia. Psychol. Med. 1–11. Advance online publication. https://doi.org/10.1017/S0033291724003088.
Yu, K., Cheung, C., Leung, M., Li, Q., Chua, S., McAlonan, G., 2010 Oct 26. Are bipolar disorder and schizophrenia Neuroanatomically distinct? An anatomical likelihood meta-analysis. Front. Hum. Neurosci. 4, 189. https://doi.org/10.3389/fnhum.2010.00189 (PMID: 21103008).
Zalesky, A., Cocchi, L., Fornito, A., Murray, M.M., Bullmore, E.D., 2012. Connectivity differences in brain networks. Neuroimage 60 (2), 1055–1062.
Zhang, L., Opmeer, E.M., Ruhé, H.G., Aleman, A., van der Meer, L.V., 2015. Brain activation during self- and other-reflection in bipolar disorder with a history of psychosis: Comparison to schizophrenia. NeuroImage: Clinical 8, 202–209. https://doi.org/10.1016/j.nicl.2015.04.010.
Zhang, X., Xu, R., Ma, H., Qian, Y., Zhu, J., 2024. Brain structural and functional damage network localization of suicide. Biol. Psychiatry 95 (12), 1091–1099. https://doi.org/10.1016/j.biopsych.2024.01.003.
Zhong, M., Liu, Z., Wang, F., Yang, J., Chen, E., Lee, E., Wu, G., Yang, J., 2024. Effects of long-term antipsychotic medication on brain instability in first-episode schizophrenia patients: a resting-state fMRI study. Front Pharmacol. 15, 1387123. https://doi.org/10.3389/fphar.2024.1387123.